European Journal of Medicinal Chemistry 214 (2021) 113222

Contents lists available at ScienceDirect

European Journal of Medicinal Chemistry

journal homepage: http://www.elsevier.com/locate/ejmech

Pyrazolo[3,4-*d*]pyrimidine-based dual EGFR T790M/HER2 inhibitors: Design, synthesis, structure–activity relationship and biological activity as potential antitumor and anticonvulsant agents

Phoebe F. Lamie [a, *], Asmaa M. El-Kalaawy [b], Noha S. Abdel Latif [c], Laila A. Rashed [d], John N. Philoppes [a]

[a] Department of Pharmaceutical Organic Chemistry, Faculty of Pharmacy, Beni-Suef University, Beni-Suef, Egypt
[b] Department of Pharmacology, Faculty of Medicine, Beni-Suef University, Beni-Suef, Egypt
[c] Department of Medical Pharmacology, Faculty of Medicine, Cairo University, Egypt
[d] Department of Medical Biochemistry and Molecular Biology, Faculty of Medicine, Cairo University, Egypt

ARTICLE INFO

Article history:
Received 16 September 2020
Received in revised form
19 January 2021
Accepted 20 January 2021
Available online 26 January 2021

Keywords:
Pyrazolopyrimidines
Triazines
Antitumor agents
Structure-activity relationship
Anticonvulsant

ABSTRACT

A new series of pyrazolo[3,4-*d*]pyrimidine/triazine hybrids **6a-r** was designed as antitumor and anticonvulsant agents. All the prepared compounds were evaluated against colon (HCT-116), breast (MCF-7) and normal human fibroblast (WI38) cell lines. The most potent derivatives against HCT-116 and MCF-7 cells were **6o** and **6q**, with IC_{50} = 4.80 and 6.50 nM, respectively, when compared to lapatinib, the reference drug (IC_{50} = 12.00 and 21.00 nM, on HCT-116 and MCF-7, sequentially). All other derivatives exhibited good to moderate cytotoxic activity. Four compounds **6f**, **6j**, **6o** and **6q** were evaluated for their EGFR T790M/HER2 inhibitory activity. They revealed 81.81–65.70% and 86.66–54.49% inhibitory activity against EGFR T790M and HER2 in a sequent. The most potent derivatives **6o** and **6q** were further estimated for cell cycle analysis showing pre G1 apoptotic activity and cell growth arrest at G2/M phase. Apoptotic marker proteins expression levels (caspase-3/7/9, Bax and Bcl-2) were measured for **6o** and **6q**. They showed pro-apoptotic effect by increasing caspase-3/7/9 protein levels and Bax/Bcl-2 ratio.

Moreover, anticonvulsant activity for the prepared compounds **6a-r** were evaluated *in vivo* using lithium-pilocarpine mice model of *Status Epilepticus*. EEG changes where recorded and MDA, GSH, GABA and glutamate were measured in brain tissue of different groups. All tested compounds revealed variable anti-epileptic effects, the most potent compounds were **6b** and **6m**. Also **6d, 6e, 6h**, **6i**, **6k, 6l** and **6n** compounds exhibited good anti-seizure activity, while compound **6j** showed the lower activity. The rest of compounds displayed a neutral activity.

1. Introduction

Protein tyrosine kinases (PTKs) enzymes play an important role in cell proliferation, metabolism and apoptosis [1,2]. Over expression or mutation of these enzymes in cancer cells results in uncontrolled cell growth [3]. Epidermal growth factor receptor protein (EGFR) is one of receptor TKs and belongs to Erb-B family [4]. It is involved in differentiation and regulation of cell growth. EGFR family is composed of structurally related RTKs such as HER1, HER2, HER3 and HER4 [5–7]. Many cancers showed to have over expression of EGFR/HER2 such as non-small cell lung cancer (NSCLC), breast, colon, prostate and ovarian cancer [3,8–11].

Therefore, there is a need to inhibit EGFR either by blocking ligand binding site to the extracellular domain or by using small molecules to interact with ATP-binding site providing EGFRIs.

A serious problem that develops in cancer patients, is the resistance to EGFR TKIs, through several mechanisms; mutation of the gatekeeper residue (T790M), upregulation of alternative signaling pathways, or bypass mechanisms using other RTKs to compensate the blockade of EGFR (e.g: HER2 amplification) [12–15].

To overcome the major resistance mechanism, mutation of the gatekeeper residue (T790M), it was found that in first generation EGFRIs (4-anilinoquinazoline based drugs such as gefitinib and

* Corresponding author.
E-mail addresses: feebi.lamey@pharm.bsu.edu.eg, feby.farag@yahoo.com (P.F. Lamie).

https://doi.org/10.1016/j.ejmech.2021.113222
0223-5234/

erlotinib), threonine was replaced with methionine but that led to steric repulsion resulting in slight different binding mode of action and loss of inhibitory activity as well as change in ATP affinity [14].

Second generation EGFRIs, contain also 4-anilinoquinazoline scaffold (afatinib and dacomitinib), they act by incorporating a Michael acceptor by covalently modifying a unique cysteine (Cys797) at EGFR-ATP binding site, but clinically they are not sufficient for patients due to severe side effects [16–18]. Finally, a third generation of EGFRIs, rociletinib and osimertinib (aminopyrimidine based structure), were developed to avoid drawbacks of generations one and two [19,20]. But due to the clinically observed elevation in blood glucose level, as a result of inhibition in insulin like growth factor 1, the production has been stopped [21,22]; only one of third generation inhibitor has FDA approval, osimertinib, showed excellent clinical results [23,24].

Screening the literature declared that many pyrazolo[3,4-*d*]pyrimidines had potent antitumor activity through inhibition of EGF tyrosine kinase as represented by compounds **I-III** in Fig. 1 [3].

Here, we present the development of new pyrazolo[3,4-*d*]pyrimidine-based series of dual EGFR mutant T790M/HER2 inhibitors as well as anticancer evaluation against human colon cancer cell line HCT-116 and human breast adenocarcinoma cell line MCF-7. As a result, structure activity relationships (SAR) were investigated. Cell cycle analysis and apoptotic biomarkers for the most active derivatives **6o** and **6q** were determined. The obtained results were compared to lapatinib, the first FDA-approved reversible dual EGFR/HER2 inhibitor for metastatic and breast cancer.

Another biological activity was studied in this research, epilepsy; it is at the same level of occurrence with breast cancer between patients in America. It affects 0.5–1% of people world-wide [25,26].

The periodic unpredictable occurrence of seizures is the most common symptoms of epilepsy. Initiation and propagation of epilepsy may be due to oxidative injury and leads to neurobiological abnormality in brain. There are no detectable drugs for prevention or curing epilepsy, they just control symptoms [27,28].

Both the classical anti-epileptic drugs (AEDs) such as phenobarbital, phenytoin, carbamazepine and valproic acid, as well as newer drugs namely, vigabatrin, zonisamide, tiagabin, topiramate and lamotrigine were reported to have promising anticonvulsant activity by reducing partial and generalized seizures [29,30].

Despite the presence of advanced AEDs, many drawbacks still facing researchers such as dose-related toxicity and adverse drug reactions (minimal brain impairment, megaloblastic anemia, aplastic anemia or hepatic failure) which may result in death, in addition to resistance of some patients to long established AEDs [31–33].

As a result, the search for new anticonvulsant drugs continues to develop safer drugs.

By inspecting lamotrigine structure, a triazine derivative, acting through prolongation of inactivation of voltage-sensitive Na^+ channel, and other related triazine analogs and pyrimidine containing compounds (methaqualone, etaqualone, mecloqualone, mebroqualone and afloqualone), it was found that the pharmacophoric elements responsible for the activity are; lipophilic aryl ring, hydrogen bond to triazine moiety, and second aryl ring that increases Van der Waal's bonding at the binding site [25,31,32,34].

Keeping in mind the previous facts, we tried to develop a new series of pyrazolo[3,4-*d*]pyrimidines hybrids with triazine scaffold aiming to have potential anticonvulsant activity as well as anticancer activity. The common features in the prepared compounds are:

1) pyrazolo[3,4-*d*]pyrimidine core combining 1,2,4-triazine ring,
2) two aromatic rings at C-3 and C-5 of triazine ring to increase the potency of the target compounds,
3) presence of many sites and groups for hydrogen bond formation,
4) substitution on phenyl rings either with electron donating groups (EDGs) or electron withdrawing groups (EWGs) to explore the electronic effect on their activities.

The rational design used to develop the new target compounds as antitumor and anticonvulsant agents is represented by Fig. 1.

2. Results and discussion

2.1. Chemistry

The intermediate and target compounds were synthesized according to the reaction pathways illustrated in Scheme 1. The key intermediate 5-amino-3-methyl-1-phenyl-1*H*-pyrazole-4-carboxamide **2** [35] was cyclized with either diethyl oxalate or diethyl malonate to yield the pyrazolopyrimidinone ethyl esters **3a** or **3b**, respectively [35,36]. Hydrazinolysis of the esters **3a&b** with hydrazine hydrate 99.99% afforded the acid hydrazide derivatives **4a&b** [35,36]. Reaction of the acid hydrazides **4a&b** with azalactone derivatives **5a-i** [37], in glacial acetic acid using anhydrous sodium acetate, gave the target triazine derivatives **6a-r**. Their IR spectra revealed absorption bands at 3395-3125 cm^{-1} due to two NH groups. Three C=O stretching vibrations appeared at the range of 1728-1667 cm^{-1}. The ^1H NMR spectra displayed a singlet signal at δ 7.21–7.40 ppm attributed to benzylidene = CH proton. Two D_2O exchangeable singlet signals were observed at δ 9.81–12.70 ppm, range, corresponding to both triazine and pyrimidine NHs. No other evidence for presence of NH_2 protons of the parent hydrazides **4a&b** was observed.

^{13}C NMR (DEPT-Q) for **6a-r** showed characteristic peak at 120.25–121.99 cm^{-1} corresponding to benzylidene = CH. Construction of the newly formed triazine ring was confirmed from ^{13}C NMR through the formation of triazine C-5 at δ 132.84–136.72 ppm and triazine C-3 at δ 146.65–158.70 ppm, beside the presence of a peak at a range of δ 160.05–166.63 ppm corresponding to triazine C=O. Another peak appeared at δ 167.26–168.60 ppm attributed to amidic C=O.

Additionally, mass spectra for compounds **6a** and **6l** revealed molecular ion peaks at m/z = 515 (16.58%) and 564 (15.75%), respectively.

***Reagents and conditions*: a**, *i)* Conc. H_2SO_4, stirring, r.t. 7 h, *ii)* NH_3; **b**, diethyl oxalate (for **3a**) or diethyl malonate (for **3b**), fusion 18 h; **c**, $N_2H_4.H_2O$ (99.99%), abs. EtOH, reflux 4–6 h; **d**, azalactone derivative **5a-i**, gl. Acetic acid, CH_3COONa, reflux 12–14 h.

Prediction of (Z/E) stereochemical configuration of target compounds 6a-r.

In addition to the used spectroscopic techniques; theoretical calculations were also adopted to establish the stereochemical orientation (*Z* or *E*-isomer) for the target compounds **6a-r**. Chem3D Pro 12.0 was used to draw both *Z* and *E*-isomers and MM2 property was selected to calculate their total energies, including, stretch, bending, stretch-bend, torsion, non-1,4 Van Der Waals, 1,4 Van Der Waals and dipole/dipole interactions. The obtained results revealed that total energy in *E*-form exceeded that in *Z*-form for target compounds **6a-i**, (Table 1). For example, compound **6b** was found to have 51.67 kcal/mol for its *Z*-form, while 62.13 kcal/mol when present in its *E*-form, (Table 1, Fig. 2). On the other hand, compounds **6j-r** are more stable in their *E*-form due to high Van Der Waals interactions of their *Z*-form. Thus, compound **6p** has 37.75 kcal/mol for its *E*-form and 963.91 kcal/mol in its *Z*-form, (Table 1, Fig. 2).

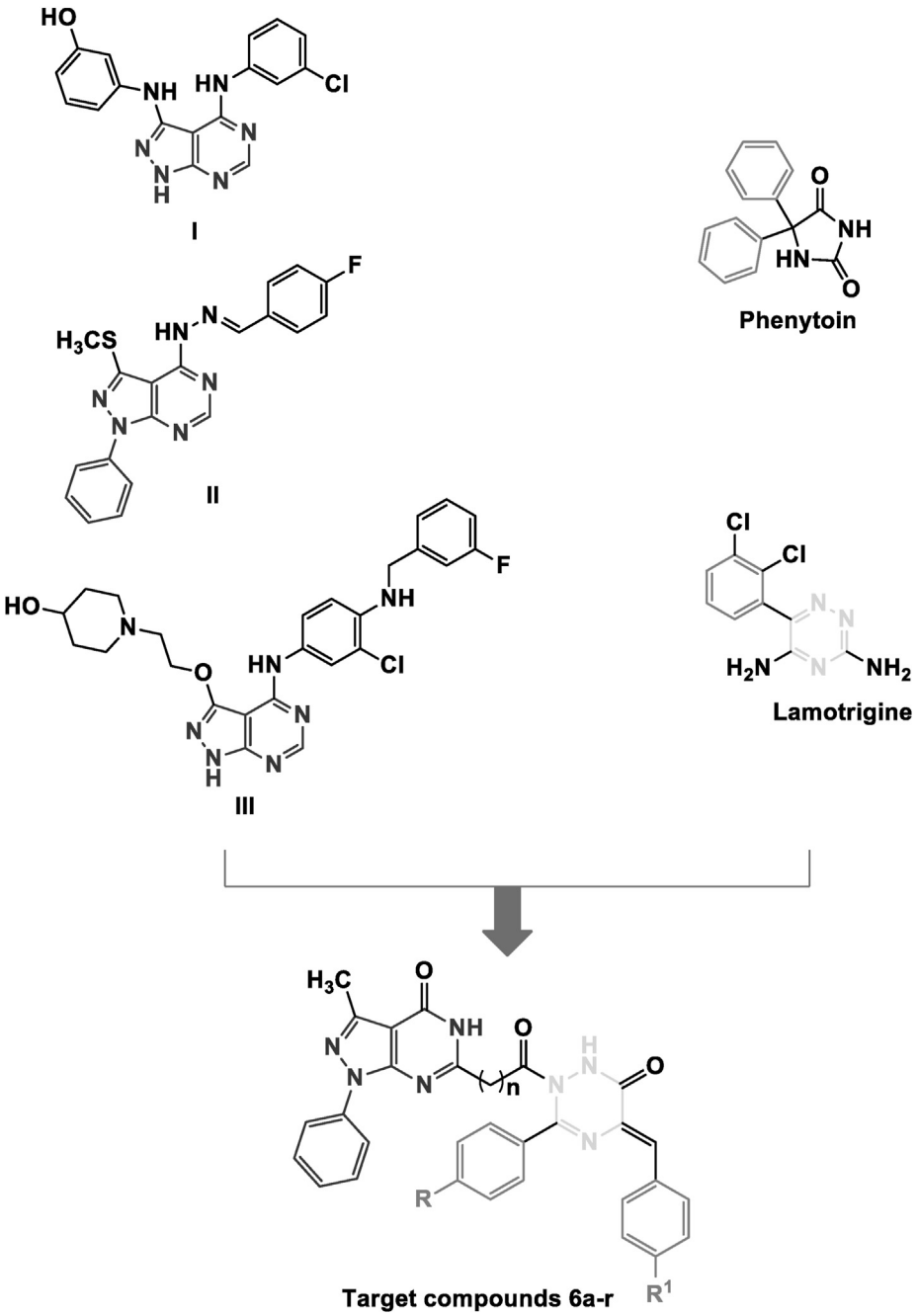

Fig. 1. Represented compounds for pyrazolo[3,4-*d*]pyrimidines with antitumor activity through EGFRI activity (**I-III**), anticonvulsant drugs and target compounds **6a-r**.

2.2. Biological evaluation

2.2.1. Antiproliferative activity

The anticancer activities of the test compounds **6a-r** were evaluated *in vitro* using MTT assay on human colon adenocarcinoma (HCT-116) and human breast adenocarcinoma (MCF-7) cell lines which overexpress EGFR and HER2 [38], in addition to normal human fibroblast (WI38) cell line. Lapatinib was used as a reference compound with IC_{50} values 12.00 nM, 21.00 nM and 45.20 nM, respectively.

*2.2.1.1. In vitro cytotoxic activity of compounds **6a-r** on HCT-116 and MCF-7 cells.* The prepared compounds **6a-r** exhibited cytotoxic activity against both HCT-116 and MCF-7 cell lines with IC_{50} values ranging from 4.8 to 93.6 nM and 6.5–126.7 nM, respectively, (Table 2). The highest cytotoxic activity was observed in compounds **6o** and **6q** (IC_{50} = 4.80 and 6.50 nM on HCT-116 and MCF-7 cell lines, sequentially). The most potent derivatives were **6f**, **6h**, **6p**, **6q** and **6r** showing IC_{50} at the range 5.60 nM–12.90 nM on HCT-116 cells. Moreover compounds **6e**, **6g**, **6i**, **6j**, **6l, 6n** and **6p** had IC_{50} of 6.90–17.80 nM on MCF-7 cell line compared to lapatinib, the reference drug.

All other pyrazolopyrimidine analogs exhibited good to moderate cytotoxic activity if compared to lapatinib. Thus, on HCT-116 cells, IC_{50} values ranged from 14.20 nM to 93.60 nM, and on MCF-7 cell line, IC_{50} values were at the range of 25.00–61.30 nM. While, compounds **6a** and **6d** showed poor cytotoxic activity on MCF-7 cell line with IC_{50} values equal to 121.30 and 126.70 nM,

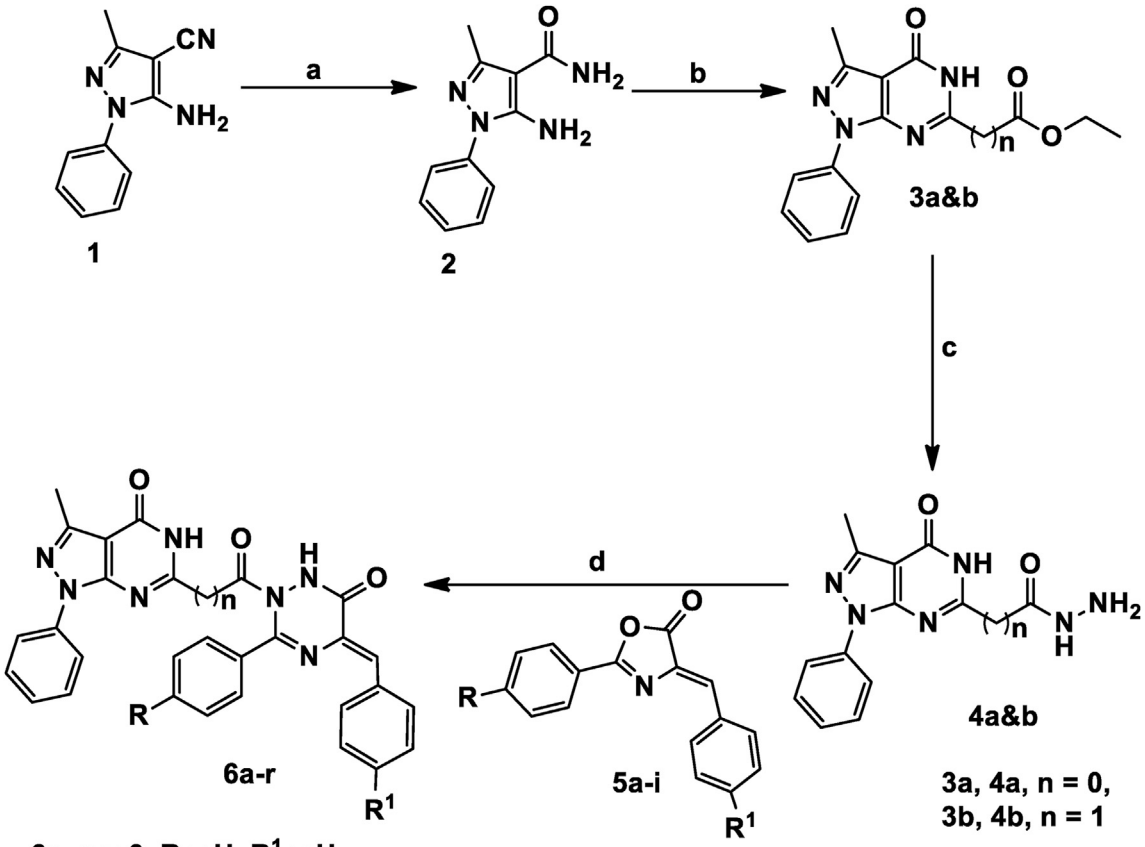

6a, n = 0, R = H, R^1 = H,
6b, n = 0, R = H, R^1 = OCH_3,
6c, n = 0, R = H, R^1 = Cl,
6d, n = 0, R = CH_3, R^1 = H,
6e, n = 0, R = CH_3, R^1 = OCH_3,
6f, n = 0, R = CH_3, R^1 = Cl,
6g, n = 0, R = Cl, R^1 = H,
6h, n = 0, R = Cl, R^1 = OCH_3,
6i, n = 0, R = Cl, R^1 = Cl,
6j, n = 1, R = H, R^1 = H,
6k, n = 1, R = H, R^1 = OCH_3,
6l, n = 1, R = H, R^1 = Cl,
6m, n = 1, R = CH_3, R^1 = H,
6n, n = 1, R = CH_3, R^1 = OCH_3,
6o, n = 1, R = CH_3, R^1 = Cl,
6p, n = 1, R = Cl, R^1 = H,
6q, n = 1, R = Cl, R^1 = OCH_3,
6r, n = 1, R = Cl, R^1 = Cl

5a, R = H, R^1 = H,
5b, R = H, R^1 = OCH_3,
5c, R = H, R^1 = Cl,
5d, R = CH_3, R^1 = H,
5e, R = CH_3, R^1 = OCH_3,
5f, R = CH_3, R^1 = Cl,
5g, R = Cl, R^1 = H,
5h, R = Cl, R^1 = OCH_3,
5i, R = Cl, R^1 = Cl

Scheme 1. Synthesis of target compounds **6a-r**.

respectively.

Additionally, tested derivatives **6a-r** were evaluated against normal human fibroblast cell line (WI38) to check their cytotoxic effect. Their IC_{50} values are represented as in Table 2. Lapatinib was used as a reference drug with IC_{50} value = 45.20 nM. The test compounds showed IC_{50} values between 12.90 nM and 110.80 nM. The most active derivatives against HCT-116 cell line, **6f** and **6o** (IC_{50} = 5.60 nM and 4.80 nM, respectively) showed IC_{50} values on normal cell (26.40 and 29.40 nM, sequentially). Moreover, compounds **6j** and **6q**, the most potent derivatives on MCF-7 cell line,

Table 1
Total energy scores (kcal/mol) for *Z*/*E* configurations of compounds **6a-r**.

Compd. No.	Total Energy (Kcal/mol)		Compd. No.	Total Energy (Kcal/mol)	
	Z-form	*E*-form		*Z*-form	*E*-form
6a	45.8921	56.4213	**6j**	963.9439	80.9645
6b	51.6796	62.1321	**6k**	969.5242	46.8927
6c	46.3922	56.7596	**6l**	964.2730	41.1748
6d	45.4974	56.4876	**6m**	962.8493	40.0806
6e	52.5985	61.8872	**6n**	968.4254	45.9470
6f	45.9910	56.5134	**6o**	963.1782	40.1955
6g	46.9821	57.3216	**6p**	963.9167	37.7555
6h	54.0893	63.0306	**6q**	969.4907	43.2380
6i	47.5257	57.6851	**6r**	964.2457	38.1421

with IC_{50} values of 6.90 nM and 6.50 nM, respectively, exerted cytotoxic activity (IC_{50} = 47.20 nM and 54.90 nM, in a sequent) on WI38 cell line.

Another seven tested compounds, **6a**, **6b**, **6g**, **6l**, **6m**, **6p** and **6q**, could be considered as safe derivatives for normal cells. Their detectable IC_{50} values were in the range of 49.50 nM−110.80 nM.

*2.2.1.2. Structure activity relationships (SAR) of cytotoxic activity of compounds **6a-r**.* In this study, a novel series of pyrazolopyrimidine/triazine hybrids **6a-r** was synthesized. The prepared compounds characterized by presence of aryl ring at triazine C-3/5 and/or *p*-substituted aryl ring carrying either electon donating group (EDG) such as methyl group at triazine C-3 or methoxy group at triazine C-5 or electon withdrawing group (EWG) like Cl at triazine C-3/5.

Additionally, triazine ring was attached to pyrazolo[3,4-*d*]pyrimidine through carbonyl spacer (**6a-i**) or carboxymethyl spacer (**6j-r**).

By inspecting *in vitro* cytotoxic activity results of the prepared compounds **6a-r** against HCT-116 and MCF-7 cell lines, and comparing them with the reference drug used, lapatinib, some points can be highlighted, (Fig. 3).

For compounds **6a-i**:

i) Improvement of cytotoxic activity of both HCT-116 and MCF-7 cell lines was achieved in compounds decorated by EWG at one of the two aryl rings (**6g**, IC_{50} = 13.90 and 12.30 nM) or at the two rings (**6i**, IC_{50} = 15.00 and 17.80 nM).
ii) Presence of two aryl rings at triazine C-3 and C-5 (**6a**), increased HCT-116 inhibitory activity (IC_{50} = 14.70 nM) if compared to lapatinib (IC_{50} = 12.00 nM), while caused sharp decrease in MCF-7 inhibitory activity (IC_{50} = 120.30 nM) compacting to lapatinib (IC_{50} = 21.00 nM).

Moreover, Combination between EWG and EDG at triazine C-3/5 aryl rings of (**6f**, IC_{50} = 5.60 and 59.30 nM) and (**6h**, IC_{50} = 12.90 and 32.90 nM), led to increase inhibitory activity of HCT-116 rather than MCF-7.

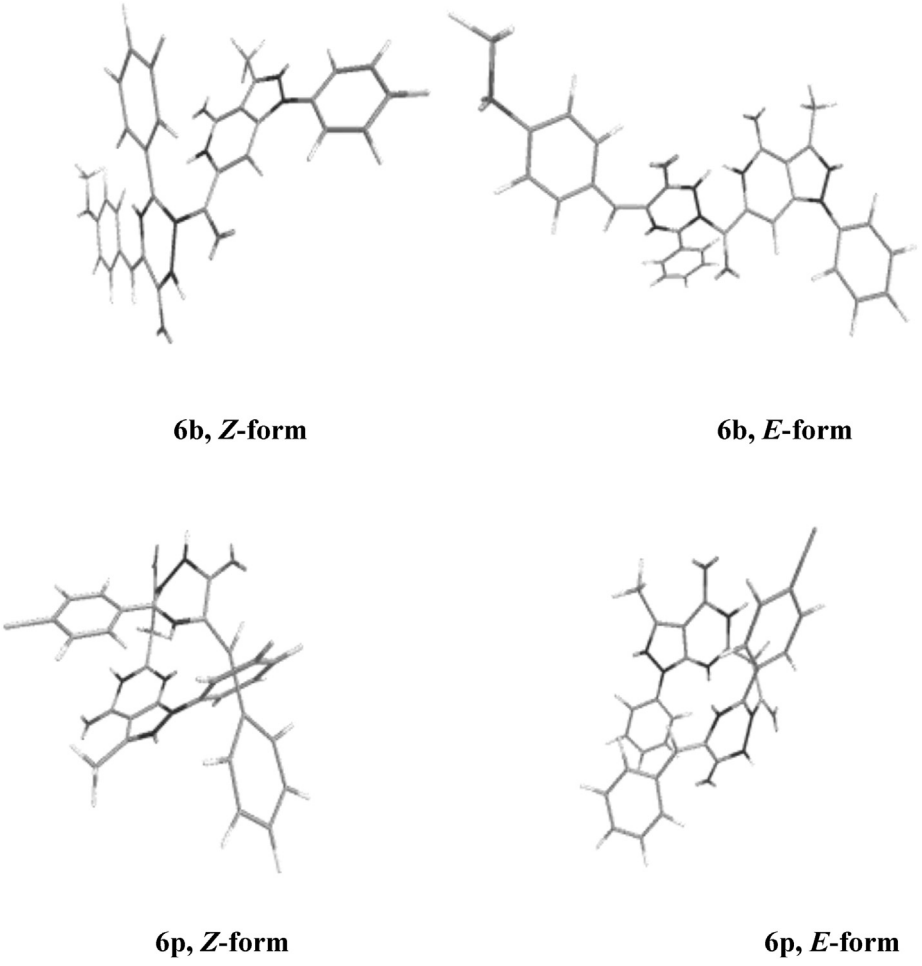

Fig. 2. Theoretical MO calculations for *Z*/*E* configuration for compounds **6b** and **6p**.

Table 2
Cytotoxic activity of tested compounds **6a-r** and reference drug, lapatinib, on HCT-116, MCF-7 and WI38 cell lines.

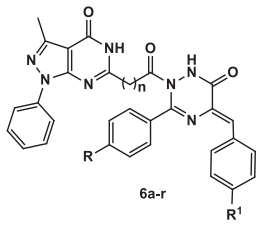

Compound no.	n	R	R^1	IC_{50} results (nM) [a]Mean ± SD		
				HCT-116	MCF-7	WI38
6a	0	H	H	14.70 ± 0.41	120.30 ± 3.76	49.50 ± 0.97
6b	0	H	OCH_3	52.10 ± 1.48	61.30 ± 1.50	97.70 ± 3.87
6c	0	H	Cl	28.10 ± 1.44	44.30 ± 0.80	31.80 ± 0.64
6d	0	CH_3	H	46.50 ± 1.32	126.70 ± 3.46	24.50 ± 0.69
6e	0	CH_3	OCH_3	37.70 ± 1.84	17.30 ± 3.05	36.80 ± 0.47
6f	0	CH_3	Cl	5.60 ± 0.25	59.30 ± 2.20	26.40 ± 0.59
6g	0	Cl	H	13.90 ± 0.49	12.30 ± 0.91	55.00 ± 1.17
6h	0	Cl	OCH_3	12.90 ± 0.48	32.90 ± 1.40	25.00 ± 0.35
6i	0	Cl	Cl	15.00 ± 0.30	17.80 ± 0.98	19.30 ± 0.80
6j	1	H	H	68.90 ± 2.18	6.90 ± 1.40	47.20 ± 1.87
6k	1	H	OCH_3	14.20 ± 0.41	31.90 ± 0.90	17.20 ± 0.54
6l	1	H	Cl	93.60 ± 2.58	7.80 ± 0.20	110.80 ± 2.13
6m	1	CH_3	H	18.20 ± 0.48	25.00 ± 1.62	85.60 ± 3.67
6n	1	CH_3	OCH_3	26.40 ± 0.31	8.00 ± 0.30	18.60 ± 0.83
6o	1	CH_3	Cl	4.80 ± 0.10	49.80 ± 1.70	29.40 ± 1.13
6p	1	Cl	H	10.30 ± 0.20	12.40 ± 0.80	80.20 ± 2.99
6q	1	Cl	OCH_3	12.90 ± 0.54	6.50 ± 0.10	54.90 ± 2.16
6r	1	Cl	Cl	7.20 ± 0.10	35.00 ± 1.60	12.90 ± 0.99
Lapatinib	–	–	–	12.00 ± 0.48	21.00 ± 0.54	45.20 ± 0.96

[a] All experiments were repeated in triplicate.

iii) Existence of two aryl rings *para* substituted with EDG (**6e**, IC_{50} = 37.70 and 17.30 nM), resulted in decreasing HCT-116 inhibitory activity, while increasing MCF-7 inhibitory activity.
iv) Reduction in inhibitory activity of both HCT-116 and MCF-7 cell lines was observed in compounds bearing one aryl ring and one *p*-substituted aryl ring with EDG or EWG as in **(6b,** IC_{50} = 52.10 and 61.30 nM), **(6c**, IC_{50} = 28.10 and 44.30 nM) and (**6d**, IC_{50} = 46.50 and 126.70 nM).

For compounds **6j-r**:

i) Highest cytotoxic activity against both HCT-116 and MCF-7 cell lines was observed in compounds (**6p,** IC_{50} = 10.30 and 12.40 nM) and **(6q,** IC_{50} = 12.90 and 6.50 nM). They are characterized by presence of either EWG at one of the two aryl rings or their presence together at the two rings.

Very slight reduction in HCT-116 and MCF-7 inhibitory activity was observed in (**6m**, IC_{50} = 18.20 and 25.00 nM), which has EDG at one of its two aryl rings.

ii) Increased HCT-116 inhibitory activity and decreased MCF-7 inhibitory activity were displayed in compounds bearing one aryl and other *p*-substituted aryl ring with EDG (**6k**, IC_{50} = 14.20 and 31.90 nM), two aryl groups carrying EDG and EWG (**6o**, IC_{50} = 4.80 and 49.80 nM) or two aryl groups with EWG (**6r,** IC_{50} = 7.20 and 35.00 nM).
iii) For decreasing inhibitory activity of HCT-116 cell line and increasing inhibitory activity of MCF-7 cell line, two aryl rings (**6j,** IC_{50} = 68.90 and 6.90 nM) or one aryl ring substituted with EWG (**6l**, IC_{50} = 93.60 and 7.80 nM) as well as two *p*-substituted aryl rings with EDG as in (**6n,** IC_{50} = 26.40 and 8.00 nM) were observed.

Finally, we can conclude that, compounds with carboxymethyl spacer (**6j-r**) were of higher activity than those with carbonyl spacer (**6a-i**) on both HCT-116 and MCF-7 cell lines. Thus between all the tested compounds, compounds **6o** and **6q** exhibited the highest cytotoxic activity on HCT-116 and MCF-7 with IC_{50} values 4.8 and 6.5 nM, respectively with 2.5- and 3.2-fold higher than that of the reference compound lapatinib (IC_{50} = 12.00 nM and 21.00 nM on HCT-116 and MCF-7, sequentially).

It is worth to notice that both compounds **6o** and **6q** had *p*-chlorophenyl moiety at triazine C-3 or C-5 beside the presence of carboxymethyl spacer at pyrazolopyrimidine C-6.

2.2.2. Detection of apoptosis and in vitro DNA-flow cytometry

The most two potent compounds **6o** and **6q** on HCT-116 and MCF7 cell lines were selected to determine their effect on cell cycle progression and apoptosis. HCT-116 and MCF-7 cells were treated with either **6o** or **6q**, respectively, at their IC_{50} concentrations for 24 h. Then, flow cytometry was used to analyze the DNA content and compared to control experiment (without treatment). Deep sight to flow cytometric analysis showed that treatment HCT-116 and MCF-7 cells with compounds **6o** and **6q**, sequentially, led to pre G1 apoptosis denoted by increase in cell population (17.35% and 22.12%, respectively), compared to the control (2.02% and 1.49%, sequentially), (Fig. 4, Table 3).

Moreover, it was observed that G2/M cell growth arrest appeared upon treatment with **6o** and **6q**, 2.98- and 11.97-fold increase compared to the control HCT-116 and MCF-7 cells, respectively, (Fig. 5).

In conclusion, the two selected compounds **6o** and **6q** showed pre G1 apoptotic activity and cell growth arrest at G2/M phase.

Compound **6q** (4-methoxyarylidine/4-chlorophenyl derivative), showed higher apoptotic activity on MCF-7 cells than **6o** (4-chloroarylidine/4-tolyl derivative) on HCT-116 cells.

2.2.3. FITC-annexin V-staining for in vitro identification of apoptosis

To further confirm that accumulation of cells which was observed in pre G1 phase was due to apoptosis, FITC-annexin v-staining technique was used. Thus, HCT-116 and MCF-7 cells were treated with compounds **6o** and **6q**, respectively for 24 h, then analyzed using PI and FITC-annexin V-stain (Fig. 6). It was observed that both early apoptosis (Q4) and late apoptosis (Q2) stages in HCT-116 cells treated with compound **6o** increased from 0.34% (control, with no treatment) to 10.37% (30.79-fold increase), and from 1.31% (control) to 2.72% (2-fold increase), respectively. Moreover, in MCF-7 cells treated with **6q**, late apoptosis was significantly increased from 0.47% (control) to 13.86% (29.48-fold increase), and in early apoptosis, increased from 0.84% (control) to 4.98% (5.6-fold increase).

The results in this experiment were in accordance with that obtained from the previous one (flow cytometry). That confirms the cytotoxic effect of compounds **6o** and **6q** through their apoptotic activities (Fig. 7).

2.2.4. In vitro ELISA immunoassay measurement of apoptotic marker proteins expression levels (caspase3/7/9, Bax and Bcl-2)

The apoptotic activity of compounds **6o** and **6q** was further investigated by measuring the induction of apoptosis of protein biomarkers, caspase-3/7/9, Bax and Bcl-2 after 24 h treatment of HCT-116 and MCF-7 cells with compounds **6o** and **6q**, respectively, at their IC_{50} values. Then, the obtained results were compared with

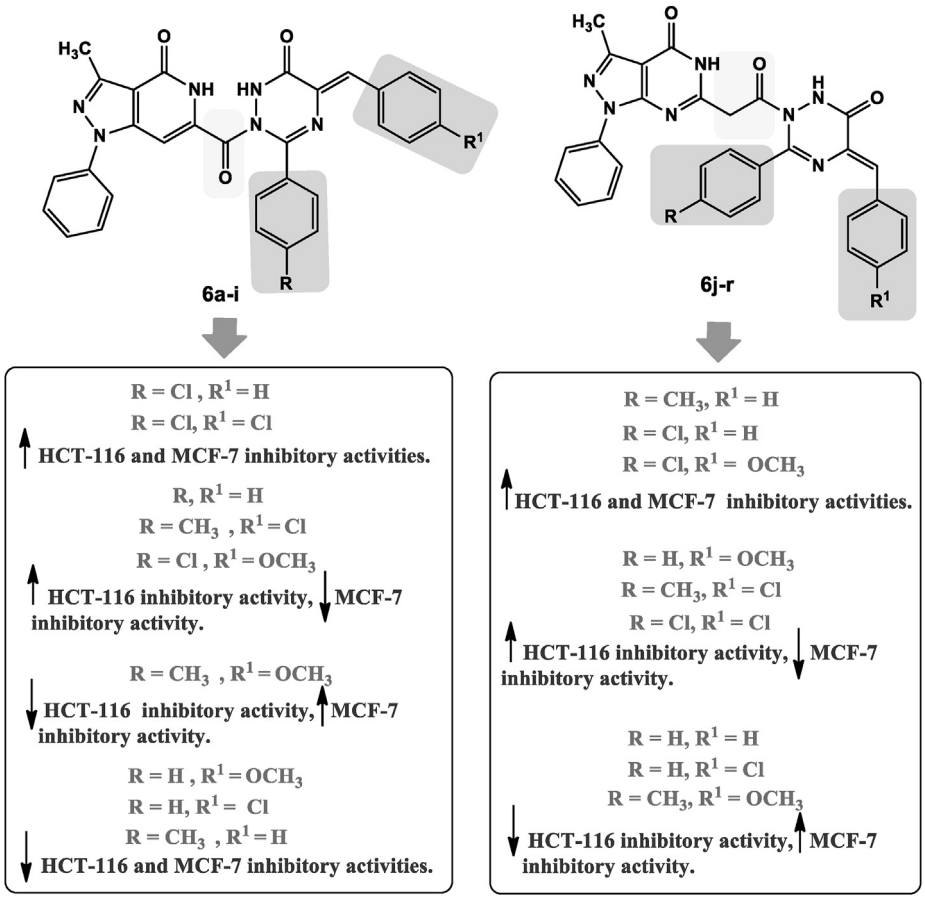

Fig. 3. Representative diagram for SAR of test compounds **6a-r**.

control HCT-116 and control MCF-7 cells. Activation of caspase-3/7 (due to both intrinsic and extrinsic factors) and caspase-9 (due to intrinsic factors) leading to cell death as a result of DNA fragmentation.

It was observed that compound **6o** increased the level of caspase-3/7/9 by 18.5-, 20- and 16.5-fold, respectively, compared to the untreated control HCT-116 cells. While, compound **6q** increased the level of caspase-3/7/9 by 12-, 7.9- and 22.9-fold, sequentially, compared to the untreated control MCF-7 cells.

Tumor cells try to resist apoptosis by increasing the expression of anti-apoptotic Bcl-2 protein level and decreasing the expression of pro-apoptotic Bax protein level.

Treatment of HCT-116 and MCF-7 cells with compounds **6o** and **6q**, respectively, resulted in up regulation in pro-apoptotic protein, Bax level by 6.9- and 5.6-fold, respectively, compared to the control HCT-116 and MCF-7 cells.

On the other hand, down regulation in anti-apoptotic protein, Bcl-2 was observed in HCT-116 and MCF-7 cells treated with **6o** and **6q**, respectively, by decreasing levels of Bcl-2 by 3.8- and 3.4-fold, sequentially, compared to control cells HCT-116 and MCF-7.

Finally, we can conclude that the two pyrazolopyrimidine derivatives **6o** and **6q** showed pro-apoptotic effect through increasing protein levels of caspase-3/7/9 and Bax/Bcl-2 ratio, (Table 4, Fig. 8).

From the results listed in Table 5, it was observed that compounds **6o** (76.97%, 72.61%), **6q** (81.81%, 86.66%) & **6j** (76.35%, 83.61%) had good inhibitory activities on both EGFR and HER2 enzymes, respectively. While, compound **6f** (65.70%, 54.49%) showed moderate inhibitory activities on both EGFR and HER2 enzymes, sequentially.

The inhibitory activities may be attributed to the substitution on phenyl ring at triazine C-3 and C-5. Thus, unsubstituted phenyl rings at C-3 and C-5 (**6j**), or *para* substituted phenyl rings with EDG (CH_3/OCH_3) or EWG (Cl) in carboxy methyl derivatives (**6o** and **6q**), increased inhibitory activity rather than presence of EDG (CH_3) and EWG (Cl) on phenyl rings of triazine scaffold in carboxy derivative (**6f**).

As a result, kinase IC_{50} for the selected compounds **6f**, **6j**, **6o** and **6q** was determined. Four concentrations (0.01 μM, 0.1 μM, 1 μM and 10 μM) were measured to determine their IC_{50} values. The order of reactivity against EGFR was **6q** (0.22 μM) > **6o** (0.42 μM) > **6j** (0.65 μM) > **6f** (1.88 μM), and that towards HER2 was **6o** (0.63 μM) > **6q** (0.86 μM) ≈ **6j** (0.87 μM) > **6f** (11.21 μM). Subsequently, the three compounds **6j**, **6f** and **6q** were potent as EGFR/HER2 inhibitors.

2.2.5. *In vitro enzyme inhibitory activity assay*

To identify new pyrazolopyrimidine derivatives with dual EGFR/HER2 inhibitory activities, the most potent derivatives on HCT-116 and/or MCF-7 (**6f**, **6j**, **6o** and **6q**) were selected for further *in-vitro* enzyme investigations on EGFR and HER2 at 10 μM.

2.2.6. *In vivo anticonvulsant activity results*

In vivo anticonvulsant activity of the tested compounds was evaluated using lithium-pilocarpine model of *Status Epilepticus* in relation to untreated SE group, phenytoin and lamotrigine as reference anti-epileptic drugs.

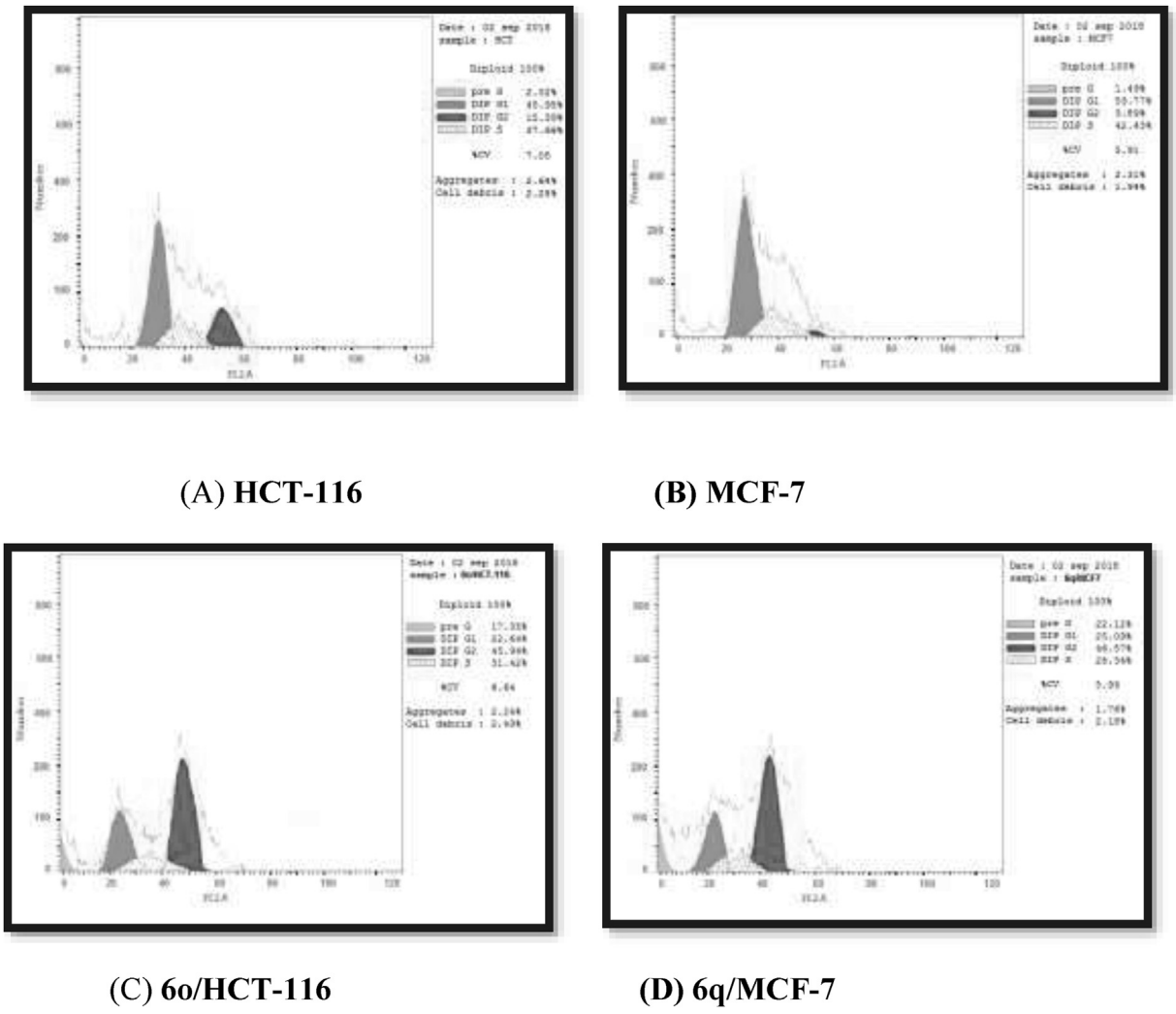

Fig. 4. Flow cytometry analysis of the most active compounds **6o** and **6q** on HCT-116 and MCF-7, respectively for 24 h. **(A)** control HCT-116 cells, **(B)** control MCF-7 cells, **(C)** HCT-116 cancer cells treated with compound **6o** (4.80 nM), **(D)** MCF-7 cancer cells treated with compound **6q** (6.50 nM).

Table 3
Cell cycle analysis after treatment with compounds **6o** and **6q** at their IC_{50} values (4.80 nM) and (6.50 nM), respectively for 24 h, compared with control HCT-116 and control MCF-7.

Compound	Results			
	%Pre-G1	%G1	%S	%G2/M
6o/HCT-116	17.35	22.64	31.42	45.94
6q/MCF-7	22.12	25.09	28.34	46.57
cont. HCT-116	2.02	46.95	37.66	15.39
cont. MCF-7	1.49	53.77	42.34	3.89

2.2.6.1. Effect of the tested compounds on EEG recording changes. The mean changes in different EEG recording of mice treated by different compounds and % change from the untreated *Status Epilepticus* (SE) group were listed in Tables 5 and 6 and represented by Fig. 9.

In the present study, the untreated SE group had significant changes ($p < 05$) when compared to the normal control group in all EEG recording except theta and alpha waves as there was non-significant effects ($p > 05$) as shown in Table 6.

In comparison with the untreated SE group; all groups administered the tested compounds revealed significant change ($p < 05$) in the mean power frequency spectral edge frequency, amplitude, amplitude density, power, total power, delta and beta waves as demonstrated in Tables 5 and 6 Also Compounds **6i** and **6n** significantly increased ($p < 05$) total power by 37.32% and 33.82%, respectively, when compared to the untreated SE group as presented in Table 7.

Compounds **6b** and **6m** showed more profound improvement similar to the group received lamotrigine evidenced by non-significant difference ($p > 05$) in the mean of power frequency, amplitude, delta waves when compared to mice received lamotrigene. Moreover mice administered the compound **6m** showed potent improvement in spectral edge frequency and beta waves as there was no significant change ($p > 05$) when compared to the group received lamotrigine as shown in Tables 6 and 7

2.2.6.2. Effects of the tested compounds on biochemical parameters. In the current study, the untreated SE group had significant changes ($p < 05$) when compared to the normal control group in all biochemical investigations; MDA, GSH, GABA and glutamate levels that measured in the mice brain tissue.

Also, all groups received the tested compounds indicated significant improvement ($p < 05$) in MDA, GSH, GABA and glutamate levels in the mice brain tissue in relation to the untreated SE group

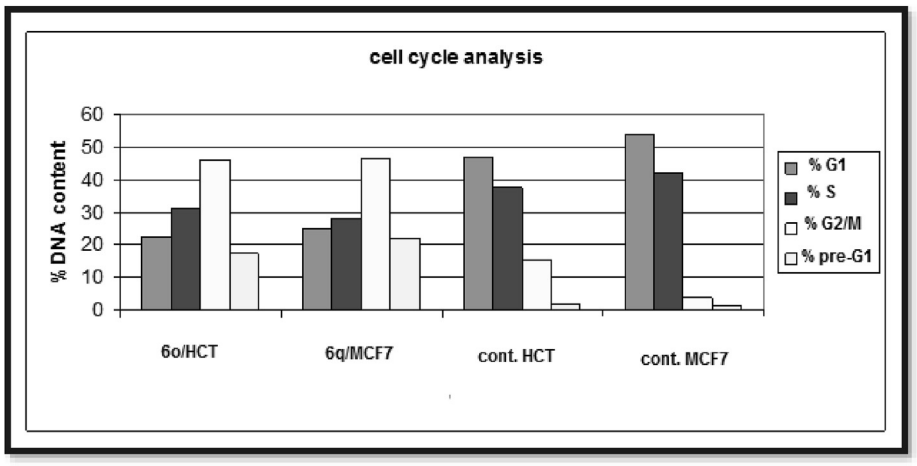

Fig. 5. Graphical representation of cell cycle analysis of compounds **6o** and **6q** compared with control cells.

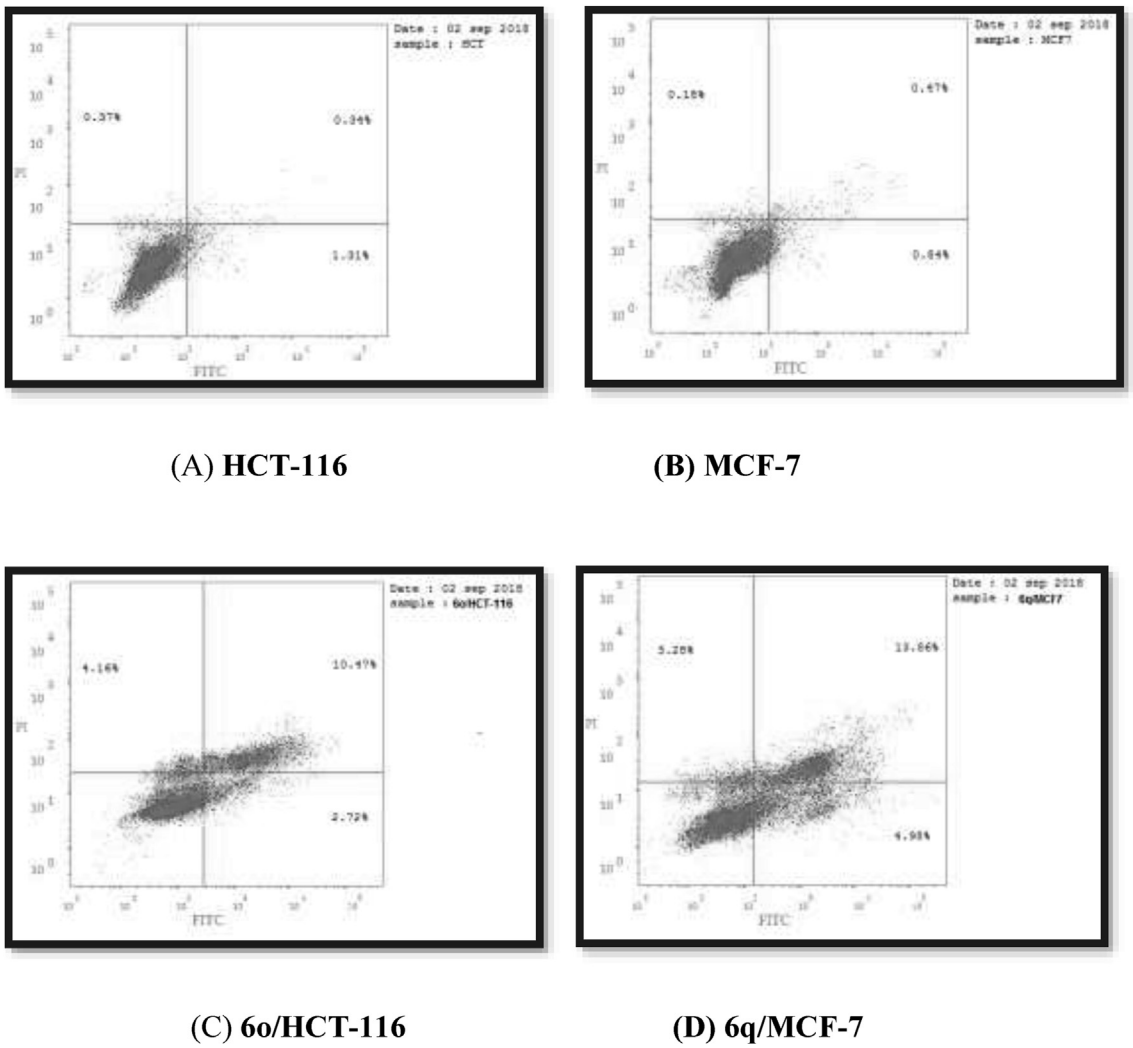

Fig. 6. FIT-annexin-V and PI staining of HCT-116 and MCF-7 cells after treatment with compounds **6o** and **6q**, respectively, and as control without treatment.

as presented in Table 8.

Moreover all groups administered the tested compounds significantly reduced lipid peroxidation ($p < 05$) evidenced by significant reduction of MDA as compared to the untreated SE group and non-significant change ($p > 05$) when compared to groups received phenytoin and lamotrigine. MDA level was

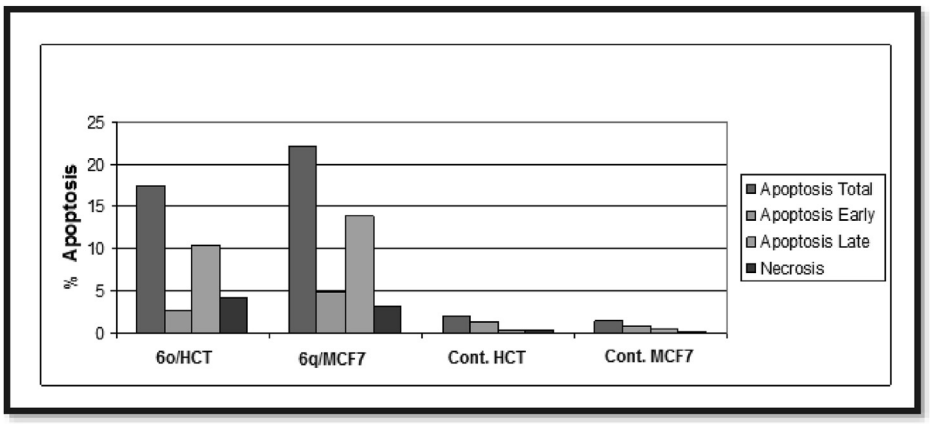

Fig. 7. Graphical representation of % apoptotic cell in case of treatment with compounds **6o** and **6q** on HCT-116 and MCF-7 cells, sequentially, against their control.

Table 4
Protein expression level of apoptotic biomarkers caspase 3/7/9, Bax and Bcl-2 in HCT-116 and MCF-7 cells after treatment with compounds **6o** (4.80 nM) and **6q** (6.50 nM), respectively, for 24 h.

Compound	Protein expression level conc. (pg./mL)				
	Caspase- 3	Caspase-7	Caspase-9	Bax	Bcl-2
6o	324 ± 11.3	0.7246 ± 19.71	8.57 ± 16.22	258.4 ± 6.97	2.55 ± 0.26
6q	176.26 ± 6.71	0.8777 ± 7.71	10.29 ± 22.80	237.4 ± 5.61	3.09 ± 0.29
Control HCT-116	17.489 ± 0.62	0.03675 ± 1	0.52 ± 1	37.03 ± 1	9.70 ± 1
Control MCF-7	14.35 ± 0.47	0.1138 ± 1	0.45 ± 1	42.28 ± 1	10.45 ± 1

obviously decreased in groups administered compounds **6a**, **6d**, **6h**, **6i**, **6k**, **6l**, **6m and 6n** by 72.13%, 66.18%, 67.54%, 63.24%,66.91%, 74.39%, 69.74% and 69.49%, respectively, in relation to untreated SE group, beside non-significant change ($p > 05$) with respect to the normal control group.

Additionally GSH level in the groups received all tested compounds was significantly increased ($p < 05$) as compared to the untreated SE group. Also there was non-significant change ($p > 05$) in relation to the group received phenytoin except compounds **6j** and **6n**; and non-significant change ($p > 05$) as compared to lamotrigine group except **6g**, **6j**, **and 6n**. The improvement of GSH level was more evident with **6a**, **6c**, **6d**, **6h**, **6l**, **6m**, **6p**, **6q** and **6r** as it increased by 154.11, 174.47%, 173.91%, 150.97%, 170.04%, 188.85%, 191.86%, 179.51% and 146.06%, respectively, in comparison with the untreated SE group, added to that there was non-significant change ($p > 05$) in relation to normal control group as listed in Table 8.

Also in the present study all groups administered the tested compounds revealed a significant increase ($p < 05$) in GABA concentration (inhibitory neurotransmitter). Added to that, all compounds except **6a**, **6d**, **6f**, **6j** and **6o** showed better improvement in GABA concentration; similar to phenytoin as there is no significant change ($p > 05$). While all compounds except **6j** and **6p** demonstrated non-significant change in GABA level ($p > 05$) as compared to the group administered lamotrigine. Compound **6k** profoundly increased GABA level by 104.31% in relation to untreated SE group and there was non-significant change ($p > 05$) in comparison with the normal control group (Table 8).

In addition, all tested compounds exhibited significant reduction ($p < 05$) in glutamate level (excitatory neurotransmitter) in relation to the untreated SE group. moreover, glutamate level in the groups administered compounds **6b**,**6d**,**6e**,**6h**,**6k**, **6l** and **6m** not only significantly reduced ($p < 05$) as compared to the untreated SE group but also showed non-significant change ($p > 05$) when compared to mice received phenytoin and lamotrigine. Also compounds **6b**, **6d**, **6k**, **6l** and **6m** exhibited potent decrease in glutamate concentration by 76.21%, 72.91%, 75.98%, 76.98% and 82.89%, respectively, with non-significant change ($p > 05$) as compared to normal control group as shown in Table 8.

Accordingly, compounds **6b** and **6m** displayed potent anti-epileptic activity. Also, **6d, 6e, 6h**, **6i**, **6k, 6l** and **6n** showed a good anti-seizure activity, while compound **6j** revealed the lower activity. Rest of compounds exhibited neutral activity.

2.3. ADME study

2.3.1. In silico ADME prediction

The most active derivatives against HCT-116 and MCF-7 cell lines **6o** and **6q**, respectively, and the reference lapatinib were subjected to *in silico* ADME prediction study to indicate their pharmacokinetic properties such as absorption, distribution, metabolism and excretion and comparing them with lapatinib, (Table 9). Thus, the two target derivatives **6o** and **6q** showed good intestinal absorption values 96.59% and 96.67%, sequentially, which are nearly equal to lapatinib (96.86%).

Moreover, moderate permeability was observed for **6o**, **6q** and lapatinib toward *in vitro* human colorectal carcinoma cells (CaCo-2) (21.81, 21.68 and 17.99, respectively). While, low permeability was appeared for the latter compounds towards *in vitro* Madin Darby Canine Kidney cells (MDCK). Compounds **6o** and **6q** exerted strong bound effect to plasma protein (91.15% and 91.22%, in a sequent) as well as lapatinib (97.56%). Moreover, the target compounds **6o** and **6q** couldn't penetrate the CNS because they had low absorption into the CNS and their predicted blood brain barrier (BBB) values were less than 0.40.

Maximum skin permeability was observed for the target derivatives **6o** and **6q** and also for the reference drug which ranged from −2.91 to −2.32. From the obtained results, we concluded that the target derivatives **6a** and **6q** had good predictable pharmacokinetic properties.

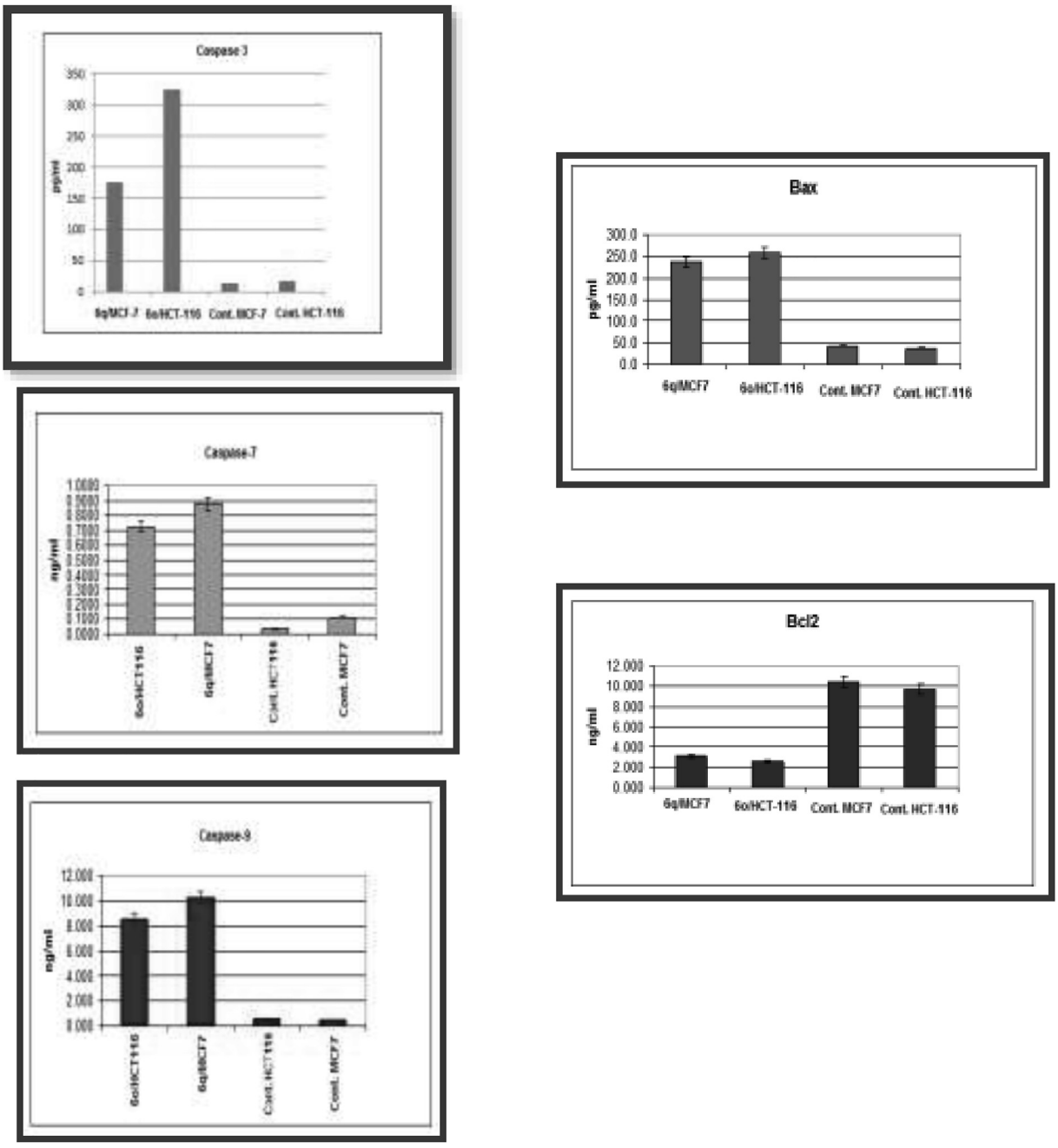

Fig. 8. Graphical representation of apoptotic biomarkers protein expression level (Caspase-3/7/9), Bax and Bcl-2 after treatment with compounds **6o** and **6q** at their IC_{50} for 24 h using ELISA immunoassay technique.

2.3.2. Predicted pharmacokinetic properties

A molecule with high bioactivity should have scores more than 0.00. While, those with values −0.50 to 0.00, exhibited moderate biological activities. The compound classified as biologically inactive if its obtained score was less than −0.50.

By inspecting data listed in Table 10, it was revealed that compounds **6o** and **6q** had moderate activity on GPCR ligand affinity and kinase inhibitory activity. Additionally, they had certain activity to act as protease inhibitor and enzyme inhibitor. Whereas, they gave low scores when ion channel modulator and nuclear receptor ligand parameters were tested. Lapatinib showed good biological activity as kinase inhibitor and moderate activity for all the other remaining tested parameters.

3. Conclusion

In an attempt to overcome the resistance against EGFR inhibitors, a new series of pyrazolo[3,4-*d*]pyrimidine-based dual EGFR T790M/HER2 was developed. All the prepared compounds **6a-r** were screened for antitumor activity against two cell lines, colon (HCT-116) and breast (MCF-7), in which EGFR is overexpressed, and on human fibroblast cells (WI38). The tested derivatives showed good to moderate activity. The highest cytotoxic activity on HCT-116 and MCF-7 cells were observed in compounds **6o** and **6q** with IC_{50} value of 4.80 and 6.50 nM, respectively, if compared with reference drug lapatinib ($IC_{50} = 12.00$ and 21.00 nM on HCT-116 and MCF-7, sequentially). Both **6o** and **6q** shared in

Table 5
% inhibitory effect 10 μM and IC_{50} (μM) values of compounds **6f**, **6j**, **6o** and **6q** and the reference lapatinib (10 μM) on EGFR T790M and HER2 kinase activities.

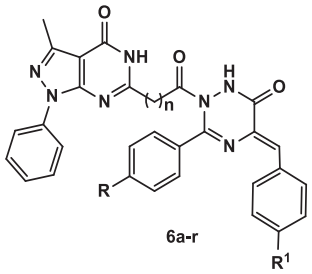

Compd. no.	N	R	R^1	% inhibition (10 μM)		IC_{50} (μM)	
				EGFR-T790M	HER2	EGFR-T790M	HER2
6f	0	CH_3	Cl	65.70%	54.49%	1.8872	11.2114
6j	0	H	H	76.35%	83.61%	0.6556	0.8723
6o	1	CH_3	Cl	76.97%	72.61%	0.42225	0.6337
6q	1	Cl	OCH_3	81.81%	86.66%	0.2267	0.8657
Lapatinib (10 μM)				77%	94%		

having *p*-chlorophenyl moiety and carboxymethyl part in their structures.

The two compounds were further selected to determine their effect on cell cycle progression and apoptosis. They showed pre G1 apoptotic activity beside cell growth arrest at G2/M phase.

Moreover, it was observed that both early and late apoptosis stages in HCT-116 cells treated with **6o** showed 30.79-fold and 2-fold increase, respectively. While, compound **6q** exhibited 29.48-fold increase in late apoptosis in MCF-7 cells.

By measuring apoptotic marker protein expression levels (caspase-3/7/9, Bax and Bcl-2), the two pyrazolopyrimidine derivatives **6o** and **6q** showed pro-apoptotic effect by increasing caspase-3/7/9 protein levels and Bax/Bcl-2 ratio.

Among tested compounds, four selected derivatives **6f**, **6j**, **6o** and **6q** were selected for further *in vitro* enzyme investigations on mutant EGFR T790M and HER2. They exhibited good inhibitory activities on both the enzymes (81.81–65.70% and 86.66–54.49%, respectively). As a result, their IC_{50} on the tested enzymes were determined.

In silico ADME prediction and pharmacokinetic study for compounds **6o** and **6q** were recorded resulting in good to moderate scores.

Merging pyrazolo[3,4-*d*]pyrimidine scaffold with triazine ring in one structure encouraged us to evaluate their anticonvulsant activity, Where lithium-pilocarpine mice model of *Status Epilepticus* was used. EEG recording changes where evaluated in addition to measurement of MDA, GSH, GABA and glutamate in the brain tissue of different groups. All compounds showed anti-epileptic effects with different efficacy as the most potent compounds **were 6b** and **6m**. additionally **6d, 6e, 6h**, **6i**, **6k, 6l**, **6n** compounds displayed good anti-seizure activity, while compound **6j** showed the lower activity. Other compounds revealed a neutral activity.

4. Experimental

4.1. Chemistry

Melting points were determined using a Griffin apparatus and are uncorrected. Infrared spectra (IR) were recorded, using KBr discs, on a Shimadzu IR-435 spectrophotometer and values were represented in cm^{-1}(Faculty of Pharmacy, Cairo University). ^1H NMR and ^{13}C NMR (DEPT-Q) were carried out using the Bruker instrument at 400 MHz for ^1H NMR and 100 MHz for ^{13}C NMR spectrophotometer, (Faculty of Pharmacy, Beni-Suef University, Beni-Suef, Egypt), in DMSO-d_6, D_2O using TMS as an internal standard and chemical shifts were recorded in ppm on the δ scale using DMSO-d_6 (2.5) as a solvent. Coupling constant (*J*) values were estimated in Hertz (Hz). Splitting patterns are designated as follows: s, singlet; d, doublet, t, triplet; q, quartet; dd, doublet of doublet; m, multiplet. The electron impact (EI) mass spectra were recorded on a Hewlett Packard 5988 spectrometer (Palo Alto, CA). Microanalysis was performed for C, H, N on PerkinElmer 2400 at the Microanalytical center, Cairo University, Egypt and was within +0.4% of theoretical values. Analytical thin layer chromatography (TLC): pre-coated plastic sheets, 0.2 mm silica gel with UV indicator (Macherey-Nagel) was employed routinely to follow the course of reactions and to check the purity of products. All other reagents, solvents were purchased from the Aldrich Chemical Company (Milwaukee, WI) and, were used without further purification.

4.1.1. General procedure for synthesis of compounds *6a-r*

A mixture of the acid hydrazide **4a** or **4b** (0.01 mol), the appropriate azalactone derivative **5a-i** (0.01 mol), sodium acetate (0.02 mol) in glacial acetic acid (10 mL) was refluxed for 12–14 h (monitored by TLC). The precipitated that formed on hot was filtered, dried and crystalized from 95% ethanol to afford **6a-r**.

*4.1.1.1. (Z)-6-(5-Benzylidene-6-oxo-3-phenyl-1,2,5,6-tetrahydro-1,2,4-triazine-2-carbonyl)-3-methyl-1-phenyl-1H-pyrazolo[3,4-d] pyrimidin-4(5H)-one (**6a**).* Yellow solid; 49% yield; mp 368–370 °C; IR (KBr) 3210, 3140 (2NH), 3032 (CH-aromatic), 2928 (CH-aliphatic), 1720-1670 (3C = O) cm^{-1}; ^1H NMR (400 MHz, DMSO-d_6, δ = ppm) δ = 2.58 (s, 3H, CH_3), 7.37 (s, 1H, = CH), 7.53–7.65 (m, 7H, benzylidene H-3, H-4, H-5, pyrazolopyrimidine phenyl H-4 and phenyl H-3, H-4, H-5), 8.12 (d, *J* = 7.6 Hz, 2H, benzylidene H-2, H-6), 8.19–8.25 (m, 4H, pyrazolopyrimidine phenyl H-3, H-5, phenyl H-2, H-6), 8.39 (d, *J* = 7.6 Hz, pyrazolopyrimidine phenyl H-2, H-6), 11.20 (s, 1H, NH, D_2O exchangeable), 12.68 (s, 1H, NH, D_2O exchangeable); ^{13}C NMR (100 MHz, DMSO-d_6, δ = ppm) δ = 13.74 (CH_3), 107.19 (pyrazolopyrimidine C-3a), 121.94 (=CH), 127.31 (pyrazolopyrimidine phenyl C-2, C-6),127.47 (pyrazolopyrimidine phenyl C-4), 128.81 (benzylidene C-4), 129.45 (phenyl C-2, C-6), 129.75 (phenyl C-3, C-5), 129.82 (benzylidene C-2, C-6), 129.88 (benzylidene C-3, C-5), 131.59 (phenyl C-4), 133.09 (pyrazolopyrimidine phenyl C-3, C-5), 133.20 (phenyl C-1), 136.15 (triazine C-5), 138.48 (benzylidene C-1), 141.01 (pyrazolopyrimidine phenyl C-1), 146.82 (pyrazolopyrimidine C-7a), 150.95 (pyrazolopyrimidine C-3), 151.20 (triazine C-3), 158.11 (pyrazolopyrimidine C-6), 159.06 (pyrazolopyrimidine C=O), 160.05 (triazine C=O), 168.17 (C=O); EIMS (*m/z*) 516 (M+1, 4.50%), 515 (M^+, 16.58%), 77 (100%). Anal.Calcd for $C_{29}H_{21}N_7O_3$ (515.17): C, 67.56; H, 4.11; N, 19.02. Found: C, 67.49; H, 4.15; N, 19.13.

*4.1.1.2. (Z)-6-[5-(4-Methoxybenzylidene)-6-oxo-3-phenyl-1,2,5,6-tetrahydro-1,2,4-triazine-2-carbonyl]-3-methyl-1-phenyl-1H-pyrazolo[3,4-d]pyrimidin-4(5H)-one (**6b**).* Yellow solid; 35% yield; mp 275–277 °C; IR (KBr) 3252, 3229 (2NH), 3009 (CH-aromatic), 2924 (CH-aliphatic), 1723-1670 (3C = O) cm^{-1}; ^1H NMR (400 MHz, DMSO-d_6, δ = ppm) δ = 2.60 (s, 3H, CH_3), 3.82 (s, 3H, OCH_3), 7.05 (d, *J* = 8.4 Hz, 2H, *p*-methoxyphenyl H-3, H-5), 7.40–7.42 (m, 3H, =CH, pyrazolopyrimidine phenyl H-4 and phenyl H-4), 7.54–7.58 (m, 4H, pyrazolopyrimidine phenyl H-3, H-5, phenyl H-3 and H-5), 7.66 (d, *J* = 8.4 Hz, 2H, *p*-methoxyphenyl H-2, H-6), 8.17–8.21 (m, 4H, pyrazolopyrimidine phenyl H-2, H-6, phenyl H-2 and H-6), 10.95 (s, 1H, NH, D_2O exchangeable), 12.17 (s, 1H, NH, D_2O exchangeable); ^{13}C NMR (100 MHz, DMSO-d_6, δ = ppm) δ = 13.76 (CH_3), 55.82 (OCH_3),

Table 6
EEG recording changes in different studied groups.

EEG recording changes (Mean ± SD)					
Groups	Mean power frequency Hz	Spectral edge frequency Hz SEF (95%)	Total Power (V2)	Amplitude μV	Amplitude density μV/Hz
N	17.05 ± 1.04	48.96 ± 5.69	7.05 ± 0.78	6.49 ± 0.45	9.62 ± 0.49
SE	97.21 ± 1.95[a]	193.90 ± 4.21[a]	3.43 ± 0.15[a]	2.25 ± 0.16[a]	3.29 ± 0.08[a]
Ph	40.30 ± 1.70[a,b]	118.79 ± 8.23[a,b]	5.20 ± 0.19[a,b]	5.82 ± 0.40[b,d]	9.05 ± 0.25[b,d]
La	48.04 ± 1.46[a,b,c]	127.84 ± 3.46[a,b]	4.57 ± .48[a,b]	5.01 ± 0.11[a,b,c]	7.98 ± 0.55[a,b,c]
6a	67.81 ± 1.53[a,b,c,d]	162.27 ± 2.44[a,b,c,d]	3.88 ± 0.29[a,c]	3.76 ± 0.37[a,b,c,d]	5.87 ± 0.38[a,b,c,d]
6b	50.07 ± 0.19[a,b,c]	144.88 ± 1.32[a,b,c,d]	4.48 ± 0.17[a]	4.49 ± 0.15[a,b,c]	6.19 ± 0.24[a,b,c,d]
6c	70.41 ± 0.76[a,b,c,d]	160.40 ± 3.06[a,b,c,d]	4.10 ± 0.11[a,c]	3.96 ± 0.16[a,b,c,d]	5.83 ± 0.31[a,b,c,d]
6d	60.34 ± 1.42[a,b,c,d]	150.74 ± 2.20[a,b,c,d]	3.96 ± 0.04[a,c]	3.65 ± 0.25[a,b,c,d]	4.48 ± 0.11[a,b,c,d]
6e	65.53 ± 0.69[a,b,c,d]	157.54 ± 1.85[a,b,c,d]	4.07 ± 0.05[a,c]	4.03 ± 0.22[a,b,c,d]	5.16 ± 0.23[a,b,c,d]
6f	68.56 ± 1.70[a,b,c,d]	154.17 ± 2.35[a,b,c,d]	3.96 ± 0.12[a,c]	3.74 ± 0.23[a,b,c,d]	5.65 ± 0.25[a,b,c,d]
6g	75.02 ± 1.42[a,b,c,d]	167.54 ± 2.20[a,b,c,d]	3.78 ± 0.27[a,c]	3.48 ± 0.07[a,b,c,d]	5.80 ± 0.15[a,b,c,d]
6h	57.92 ± 1.56[a,b,c,d]	150.26 ± 1.55[a,b,c,d]	3.94 ± 0.14[a,c]	3.85 ± 0.15[a,b,c,d]	4.83 ± 0.24[a,b,c,d]
6i	60.65 ± 1.71[a,b,c,d]	152.31 ± 2.33[a,b,c,d]	4.71 ± 0.02[a,b]	4.27 ± 0.26[a,b,c,d]	5.07 ± 0.08[a,b,c,d]
6j	73.90 ± 1.62[a,b,c,d]	160.06 ± 1.46[a,b,c,d]	3.51 ± 0.23[a,c,d]	3.67 ± 0.26[a,b,c,d]	5.33 ± 0.06[a,b,c,d]
6k	58.95 ± 0.67[a,b,c,d]	151.50 ± 1.86[a,b,c,d]	4.00 ± 0.01[a,c]	3.74 ± 0.28[a,b,c,d]	4.86 ± 0.19[a,b,c,d]
6l	54.33 ± 0.70[a,b,c,d]	139.43 ± 1.71[a,b,c,d]	4.22 ± 0.10[a,c]	4.11 ± 0.12[a,b,c,d]	5.37 ± 0.44[a,b,c,d]
6m	52.27 ± 2.46[a,b,c]	137.66 ± 2.25[a,b,c]	4.23 ± 0.20[a,c]	4.29 ± 0.16[a,b,c]	6.92 ± 0.44[a,b,c,d]
6n	65.13 ± 3.69[a,b,c,d]	142.63 ± 4.03[a,b,c,d]	4.59 ± 0.21[a,b]	4.06 ± 0.18[a,b,c,d]	6.02 ± 0.14[a,b,c,d]
6o	73.49 ± 2.03[a,b,c,d]	162.61 ± 3.32[a,b,c,d]	3.34 ± 0.17[a,c,d]	3.38 ± 0.12[a,b,c,d]	5.33 ± 0.18[a,b,c,d]
6p	69.49 ± 2.21[a,b,c,d]	160.29 ± 0.73[a,b,c,d]	3.42 ± 0.23[a,c,d]	3.49 ± 0.13[a,b,c,d]	5.53 ± 0.23[a,b,c,d]
6q	69.42 ± 1.02[a,b,c,d]	154.72 ± 2.73[a,b,c,d]	3.88 ± 0.25[a,c]	3.32 ± 0.23[a,b,c,d]	5.51 ± 0.26[a,b,c,d]
6r	72.86 ± 1.72[a,b,c,d]	167.93 ± 2.27[a,b,c,d]	3.45 ± 0.30[a,c,d]	3.28 ± 0.09[a,b,c,d]	5.57 ± 0.28[a,b,c,d]
EEG recording changes (Mean ± SD)					
Groups	Power pV2	Total Power density pV2/Hz	Delta μV2/Hz	Theta μV2/Hz	Alpha μV2/Hz
N	32.49 ± 2.79	79.66 ± 3.96	63.20 ± 4.47	18.50 ± 0.64	14.34 ± 0.37
SE	5.96 ± 0.77[a]	13.88 ± 0.45[a]	9.08 ± 0.39[a]	14.12 ± 0.26	16.87 ± 0.51
Ph	25.80 ± .89[a,b,d]	66.85 ± 1.37[a,b,d]	53.20 ± 3.00[a,b,d]	16.91 ± 0.94	14.37 ± 0.54
La	22.21 ± 0.37[a,b,c]	62.03 ± 0.61[a,b,c]	47.71 ± 1.60[a,b,c]	15.83 ± 1.03	15.42 ± 0.33
6a	14.23 ± 0.47[a,b,c,d]	45.71 ± 0.78[a,b,c,d]	37.62 ± 2.07[a,b,c,d]	18.20 ± 0.64	18.96 ± 0.61
6b	19.67 ± 1.02[a,b,c]	50.70 ± 2.23[a,b,c,d]	42.58 ± 3.16[a,b,c]	18.26 ± 0.42	15.94 ± 0.67
6c	13.96 ± 0.19[a,b,c,d]	42.01 ± 0.58[a,b,c,d]	33.68 ± 1.25[a,b,c,d]	18.93 ± 0.09	20.06 ± 0.16
6d	14.53 ± 0.55[a,b,c,d]	43.05 ± 0.80[a,b,c,d]	31.04 ± 0.50[a,b,c,d]	18.64 ± 0.99	18.41 ± 0.37
6e	17.79 ± 0.42[a,b,c,d]	44.76 ± 1.08[a,b,c,d]	35.87 ± 1.29[a,b,c,d]	18.68 ± 0.76	17.71 ± 0.77
6f	15.02 ± 0.37[a,b,c,d]	42.80 ± 1.46[a,b,c,d]	32.40 ± 0.92[a,b,c,d]	19.05 ± 0.65	19.19 ± 1.23
6g	13.92 ± 0.15[a,b,c,d]	41.71 ± 0.76[a,b,c,d]	32.15 ± 1.29[a,b,c,d]	16.39 ± 5.17	21.46 ± 0.95[a,c,d]
6h	17.33 ± 0.65[a,b,c,d]	47.95 ± 1.40[a,b,c,d]	39.10 ± 1.54[a,b,c,d]	16.98 ± 0.28	16.07 ± 0.42
6i	19.42 ± 0.51[a,b,c,d]	46.34 ± 1.74[a,b,c,d]	37.57 ± 0.84[a,b,c,d]	19.93 ± 0.26	17.65 ± 1.04
6j	14.11 ± 0.26[a,b,c,d]	41.97 ± 0.29[a,b,c,d]	33.08 ± 1.70[a,b,c,d]	18.61 ± 0.98	22.52 ± 0.75[a,c,d]
6k	15.95 ± 0.13[a,b,c,d]	43.81 ± 0.59[a,b,c,d]	33.29 ± 0.46[a,b,c,d]	17.57 ± 0.71	17.30 ± 0.34
6l	18.14 ± 0.18[a,b,c,d]	48.41 ± 1.27[a,b,c,d]	38.81 ± 1.03[a,b,c,d]	16.99 ± 0.31	16.89 ± 0.04
6m	20.47 ± 0.85[a,b,c]	55.84 ± 1.71[a,b,c,d]	42.35 ± 0.97[a,b,c]	15.79 ± 0.37	15.86 ± 0.68
6n	19.01 ± 0.69[a,b,c,d]	50.61 ± 1.05[a,b,c,d]	42.02 ± 1.21[a,b,c,d]	17.95 ± 0.37	16.99 ± 0.75
6o	13.19 ± 0.70[a,b,c,d]	38.42 ± 1.22[a,b,c,d]	29.94 ± 1.41[a,b,c,d]	20.45 ± 0.69	22.26 ± 1.07[a,c,d]
6p	12.99 ± 0.18[a,b,c,d]	38.23 ± 0.54[a,b,c,d]	33.14 ± 0.66[a,b,c,d]	19.06 ± 0.68	22.75 ± 1.37[a,b,c,d]
6q	13.85 ± 0.33[a,b,c,d]	38.14 ± 1.43[a,b,c,d]	32.52 ± 0.82[a,b,c,d]	21.91 ± 1.55	21.60 ± 1.18[a,c,d]
6r	13.50 ± 0.83[a,b,c,d]	39.14 ± 0.90[a,b,c,d]	30.86 ± 1.31[a,b,c,d]	21.77 ± 1.21	22.92 ± 1.64[a,b,c,d]

Each value represents the mean ± SD.
Statistical analysis was performed using one-way ANOVA test followed by Tukey post-hoc test.
Differences between group means were considered significant at $p < 0.05$.
[a]Significantly different from normal control group value at $p < 0.05$.
[b]Significantly different from untreated SE group value at $p < 0.05$.
[c]Significantly different from phenytoin received group value at $p < 0.05$.
[d]Significantly different from lamotrigine received group value at $p < 0.05$.
N: normal control group; **SE**: untreated *Status Epilepticus* group model; **Ph**: phenytoin; **La**: lamotrigine; **6a-6r**: the tested compounds.

102.21 (pyrazolopyrimidine C-3a), 114.89 (*p*-methoxybenzylidene C-3, C-5), 121.97 (=CH), 126.88 (pyrazolopyrimidine phenyl C-2, C-6), 127.25 (pyrazolopyrimidine phenyl C-4), 128.41(*p*-methoxybenzylidene C-1), 129.73 (phenyl C-3, C-5), 131.91 (phenyl C-2, C-6), 132.00 (phenyl C-1), 133.66 (*p*-methoxybenzylidene C-2, C-6), 135.00 (triazine C-5), 135.40 (pyrazolopyrimidine phenyl C-3, C-5), 137.37 (phenyl C-4), 141.01 (pyrazolopyrimidine C-1), 143.48 (pyrazolopyrimidine C-7a), 148.29 (pyrazolopyrimidine C-3), 156.15 (triazine C-3), 157.24 (pyrazolopyrimidine C-6), 160.08 (*p*-methoxybenzylidene C-4), 162.27 (pyrazolopyrimidine C=O), 166.63 (triazine C=O), 168.38 (C=O); Anal. Calcd for $C_{30}H_{23}N_7O_4$ (545.18): C, 66.05; H, 4.25; N, 17.97. Found: C, 66.17; H, 4.15; N, 17.89.

*4.1.1.3. (Z)-6-[5-(4-Chlorobenzylidene)-6-oxo-3-phenyl-1,2,5,6-tetrahydro-1,2,4-triazine-2-carbonyl]-3-methyl-1-phenyl-1H-pyrazolo[3,4-d]pyrimidin-4(5H)-one (**6c**).* Yellow solid; 58% yield; mp 230–232 °C; IR (KBr) 3264, 3148 (2NH), 3024 (CH-aromatic), 2932 (CH-aliphatic), 1728-1670 (3C = O) cm^{-1}; ^1H NMR (400 MHz, DMSO-d_6, δ = ppm) δ = 2.58 (s, 3H, CH_3), 7.39–7.45 (m, 3H, =CH and *p*-chlorophenyl H-3, H-5), 7.53–7.66 (m, 6H, phenyl H-3, H-4, H-5, pyrazolopyrimidine phenyl H-3, H-4 and H-5), 8.12 (d, J = 7.2 Hz, 2H, phenyl H-2, H-6), 8.21 (d, J = 8 Hz, 2H, *p*-chlorophenyl H-2, H-6), 8.41 (d, J = 8.8 Hz, 2H, pyrazolopyrimidine phenyl H-2, H-6), 12.09 (s, 1H, NH, D_2O exchangeable), 12.65 (s, 1H, NH, D_2O exchangeable); ^{13}C NMR (100 MHz, DMSO-d_6, δ = ppm)

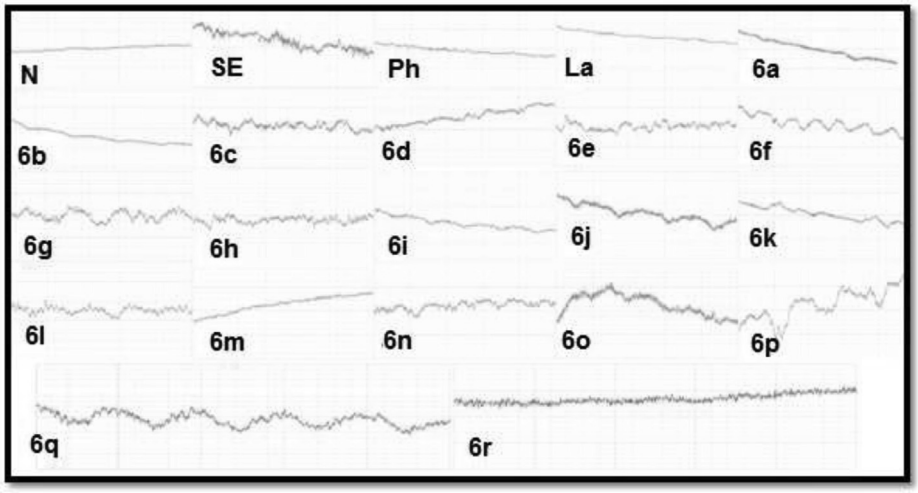

Fig. 9. EEG recording signal changes in different studied groups. **N**: normal control group; **SE**: untreated *Status Epilepticus* group model; **Ph**: phenytoin; **La**: lamotrigine; **6a-6r**: the tested compounds.

Table 7
The mean % Change of EEG recording in different groups.

% of Change From untreated SE group					
Groups	Mean power frequency Hz	Spectral edge frequency Hz SEF (95%)	Total Power (V2)	Amplitude μV	Amplitude density μV/Hz
Ph	−58.54%	−38.74%	51.60%	158.67%	175.08%
La	−50.58%	−34.07%	33.24%	122.67%	142.55%
6a	−30.24%	−16.31%	13.12%	67.11%	78.42%
6b	−48.49%	−25.28%	30.61%	99.56%	88.15%
6c	−27.57%	−17.28%	19.53%	76.00%	77.20%
6d	−37.93%	−22.26%	15.45%	62.22%	36.17%
6e	−32.59%	−18.75%	18.66%	79.11%	56.84%
6f	−29.47%	−20.49%	15.45%	66.22%	71.73%
6g	−22.83%	−13.59%	10.20%	54.67%	76.29%
6h	−40.42%	−22.51%	14.87%	71.11%	46.81%
6i	−37.61%	−21.45%	37.32%	89.78%	54.10%
6j	−23.98%	−17.45%	2.33%	63.11%	62.01%
6k	−39.36%	−21.87%	16.62%	66.22%	47.72%
6l	−44.11%	−28.09%	23.03%	82.67%	63.22%
6m	−46.23%	−29.00%	23.32%	90.67%	110.33%
6n	−33.00%	−26.44%	33.82%	80.44%	82.98%
6o	−24.40%	−16.14%	2.62%	50.22%	62.01%
6p	−28.52%	−17.33%	0.29%	55.11%	68.09%
6q	−28.59%	−20.21%	13.12%	47.56%	67.48%
6r	−25.05%	−13.39%	0.58%	45.78%	69.30%

% of Change From untreated SE group					
Groups	Power pV2	Total Power density pV2/Hz	Delta μV2/Hz	Theta μV2/Hz	Alpha μV2/Hz
Ph	332.89%	381.63%	485.90%	19.76%	−14.82%
La	272.65%	346.90%	425.44%	12.11%	−8.6%
6a	138.76%	229.32%	314.32%	28.90%	12.39%
6b	230.03%	265.27%	368.94%	29.32%	−5.51%
6c	134.23%	202.67%	270.93%	34.07%	18.91%
6d	143.79%	210.16%	241.85%	32.01%	9.13%
6e	198.49%	222.48%	295.04%	32.29%	4.98%
6f	152.01%	208.36%	256.83%	34.92%	13.75%
6g	133.56%	200.50%	254.07%	16.08%	27.21%
6h	190.77%	245.46%	330.62%	20.25%	−4.74%
6i	225.84%	233.86%	313.77%	41.15%	4.62%
6j	136.74%	202.38%	264.32%	31.80%	33.49%
6k	167.62%	215.63%	266.63%	24.43%	2.55%
6l	204.36%	248.78%	327.42%	20.33%	0.12%
6m	243.46%	302.31%	366.41%	11.83%	−5.99%
6n	218.96%	264.63%	362.78%	27.12%	0.71%
6o	121.31%	176.80%	229.74%	44.83%	31.95%
6p	117.95%	175.43%	264.98%	34.99%	34.85%
6q	132.38%	174.78%	258.15%	55.17%	28.04%
6r	126.51%	181.99%	239.87%	54.18%	35.86%

Percentage (%) changes were calculated by comparing groups received the tested compounds with the untreated SE group.
Ph: phenytoin; **La**: lamotrigine; **6a-6r**: the tested compounds.

Table 8
Biochemical analysis in different studied groups.

Parameters (Mean ± SD)				
Groups	MDA (nmol/mg protein)	GSH (mmol/mg protein)	GABA (ng/mg) protein	Glutamate (ng/mg) protein
N	8.36 ± 2.15	76.23 ± 13.15	221.63 ± 7.71	1.46 ± 0.15
SE	54.40 ± 14.59[a]	23.23 ± 2.41[a]	97.06 ± 3.98[a]	13.03 ± 0.70[a]
Ph	23.46 ± 1.80[a,b]	59.56 ± 14.78[b]	187.20 ± 2.19[a,b]	2.43 ± 0.30[b]
La	23.03 ± 3.56[a,b]	63.26 ± 9.26[b]	177.66 ± 13.65[a,b]	2.46 ± 0.32[b]
6a	15.16 ± 2.85[b]	59.03 ± 1.20[b]	156.96 ± 10.23[a,b,c]	5.43 ± 1.35[a,b,c,d]
6b	25.00 ± 1.15[a,b]	56.06 ± 3.16[a,b]	163.70 ± 14.01[a,b]	3.10 ± 0.60[b]
6c	25.30 ± 2.85[a,b]	63.76 ± 1.05[b]	169.63 ± 16.27[a,b]	6.43 ± 0.05[a,b,c,d]
6d	18.40 ± 1.27[b]	63.63 ± 6.46[b]	155.03 ± 11.75[a,b,c]	3.53 ± 0.65[b]
6e	28.96 ± 1.30[a,b]	46.00 ± 2.15[a,b]	174.36 ± 9.42[a,b]	4.20 ± 0.10[a,b]
6f	26.80 ± 1.65[a,b]	49.53 ± 1.85[a,b]	153.50 ± 6.00[a,b,c]	8.33 ± 1.76[a,b,c,d]
6g	24.33 ± 0.77[a,b]	41.90 ± 3.70[a,b,c]	183.80 ± 2.40[a,b]	7.83 ± 1.30[a,b,c,d]
6h	17.66 ± 3.25[b]	58.30 ± 3.10[b]	181.53 ± 0.95[a,b]	4.36 ± 0.30[a,b]
6i	20.00 ± 3.85[b]	56.70 ± 7.10[a,b]	169.36 ± 6.71[a,b]	5.50 ± 0.65[a,b,c,d]
6j	23.43 ± 1.75[a,b]	39.30 ± 3.30[a,b,c,d]	148.16 ± 4.60[a,b,c,d]	6.40 ± 0.10[a,b,c,d]
6k	18.00 ± 1.75[b]	54.93 ± 9.75[a,b]	198.30 ± 7.26[b]	3.13 ± 1.00[b]
6l	13.93 ± 3.65[b]	63.66 ± 2.41[b]	175.30 ± 9.26[a,b]	3.00 ± 0.96[b]
6m	16.46 ± 2.50[b]	67.10 ± 8.87[b]	185.60 ± 2.00[a,b]	2.23 ± 0.15[b]
6n	16.60 ± 1.70[b]	35.00 ± 2.32[a,b,c,d]	166.83 ± 1.55[a,b]	6.46 ± 0.20[a,b,c,d]
6o	23.03 ± 2.80[a,b]	54.50 ± 1.75[a,b]	152.16 ± 8.85[a,b,c]	8.13 ± 0.95[a,b,c,d]
6p	28.90 ± 2.40[a,b]	67.80 ± 3.81[b]	135.93 ± 3.55[a,b,c,d]	7.10 ± 0.20[a,b,c,d]
6q	27.20 ± 0.30[a,b]	64.93 ± 0.25[b]	166.50 ± 3.15[a,b]	8.33 ± 1.66[a,b,c,d]
6r	21.43 ± 3.2[a,b]	57.16 ± 0.95[b]	176.86 ± 9.45[a,b]	5.40 ± 0.70[a,b,c,d]
% of Change From untreated SE group				
Groups	MDA	GSH	GABA	Glutamate
N	–	–	–	–
SE	–	–	–	–
Ph	−56.88%	156.39%	92.87%	−81.35%
La	−57.67%	172.32%	83.04%	−81.12%
6a	−72.13%	154.11%	61.71%	−58.33%
6b	−54.04%	141.33%	68.66%	−76.21%
6c	−53.49%	174.47%	74.77%	−50.65%
6d	−66.18%	173.91%	59.73%	−72.91%
6e	−46.76%	98.02%	79.64%	−67.77%
6f	−50.74%	113.22%	58.15%	−36.07%
6g	−55.28%	80.37%	89.37%	−39.91%
6h	−67.54%	150.97%	87.03%	−66.54%
6i	−63.24%	144.08%	74.49%	−57.79%
6j	−56.93%	69.18%	52.65%	−50.88%
6k	−66.91%	136.46%	104.31%	−75.98%
6l	−74.39%	174.04%	80.61%	−76.98%
6m	−69.74%	188.85%	91.22%	−82.89%
6n	−69.49%	50.67%	71.88%	−50.42%
6o	−57.67%	134.61%	56.77%	−37.61%
6p	−46.88%	191.86%	40.05%	−45.51%
6q	−50%	179.51%	71.54%	−36.07%
6r	−60.61%	146.06%	82.22%	−58.56%

Each value represents the mean ± SD.
Statistical analysis was performed using one-way ANOVA test followed by Tukey post-hoc test.
Differences between group means were considered significant at $p < 0.05$.
[a]Significantly different from normal control group value at $p < 0.05$.
[b]Significantly different from untreated SE group value at $p < 0.05$.
[c]Significantly different from phenytoin received group value at $p < 0.05$.
[d]Significantly different from lamotrigine received group value at $p < 0.05$.
Percentage (%) changes were calculated by comparing groups received the tested compounds with untreated SE group.
N: normal control group; **SE**: untreated *Status Epilepticus* group model; **Ph**: phenytoin; **La**: lamotrigine; **6a-6r**: the tested compounds; **MDA**: malondialdehyde; **GSH**: glutathione reduced; **GABA**: gamma-aminobutyric acid.

δ = 13.73 (CH_3), 107.40 (pyrazolopyrimidine C-3a), 121.99 (=CH), 127.19 (phenyl C-1), 127.29 (pyrazolopyrimidine phenyl C-2, C-6), 127.45 (pyrazolopyrimidine phenyl C-4), 128.31 (phenyl C-2, C-6), 128.87 (*p*-chlorophenyl C-3, C-5), 129.46 (phenyl C-3, C-5), 129.57 (*p*-chlorophenyl C-2, C-6), 133.03 (*p*-chlorophenyl C-1), 133.22 (phenyl C-4), 134.72 (pyrazolopyrimidine phenyl C-3, C-5), 136.19 (*p*-chlorophenyl C-4), 136.51 (triazine C-5), 138.49 (pyrazolopyrimidine phenyl C-1), 146.85 (pyrazolopyrimidine C-7a), 150.96 (pyrazolopyrimidine C-3), 151.20 (triazine C-3), 158.10 (pyrazolopyrimidine C-6), 159.07 (pyrazolopyrimidine C=O), 160.45 (triazine C=O), 168.05 (C=O); Anal. Calcd for $C_{29}H_{20}ClN_7O_3$ (549.13): C, 63.33; H, 3.67; N, 17.83. Found: C, 63.27; H, 3.71; N, 17.85.

*4.1.1.4. (Z)-6-[5-Benzylidene-6-oxo-3-(p-tolyl)-1,2,5,6-tetrahydro-1,2,4-triazine-2-carbonyl]-3-methyl-1-phenyl-1H-pyrazolo[3,4-d] pyrimidin-4(5H)-one (**6d**).* Yellow solid; 37% yield; mp 337–339 °C; IR (KBr) 3325, 3194 (2NH), 3009 (CH-aromatic), 2924 (CH-aliphatic),1722-1673 (3C = O) cm^{-1}; ^1H NMR (400 MHz, DMSO-d_6, δ = ppm) δ = 2.36 (s, 3H, CH_3), 2.56 (s, 3H, CH_3), 7.31–7.49 (m, 2H, =CH, benzylidene H-4), 7.51–7.58 (m, 7H, benzylidene H-3, H-5, *p*-tolyl H-3, H-5, phenyl H-3, H-4, H-5), 8.04 (d, *J* = 8.4 Hz, 2H,

Table 9
Predicted *in silico* ADME properties for compounds **6o** and **6q**, and lapatinib.

Compd. No.	[a]HIA	[b]CaCo-2	[c]MDCK	[d]BPB	[e]BBB	[f]SkinP
Acceptable value	70−100% (good absorption)	˃ 90 (high permeability)		˃ 90% strong binding	˃ 0.40 CNS active compound	≥ −3
6◦	96.59	21.81	0.04	91.15	0.20	−2.71
6q	96.67	21.68	0.04	91.22	0.18	−2.91
Lapatinib	96.86	17.99	0.05	97.56	0.03	−2.32

[a] Human intestinal absorbtion (%).
[b] *in vitro* CaCo cell permeability (nm/sec).
[c] *in vitro* MDCK cell permeability (nm/sec).
[d] *in vitro* plasma protein binding (%).
[e] *in vitro* blood brain barrier penetration (C. brain/C. blood).
[f] Skin permeability.

Table 10
Predicted pharmacokinetic properties of target compounds **6o**, **6q** and lapatinib.

Compd. No.	GPCR ligand	Ion channel modulator	Kinase inhibitor	Nuclear receptor ligand	Protease inhibitor	Enzyme inhibitor
6o	−0.28	−1.07	−0.17	−0.91	−0.44	−0.38
6q	−0.32	−1.16	−0.24	−0.96	−0.46	−0.45
Lapatinib	−0.04	−0.52	0.36	−0.35	−0.21	−0.08

benzylidene H-2, H-6), 8.20 (d, J = 7.2 Hz, 2H, *p*-tolyl H-2, H-6), 8.25 (d, J = 8 Hz, 2H, phenyl H-2, H-6), 9.98 (s, 1H, NH, D_2O exchangeable), 12.65 (s, 1H, NH, D_2O exchangeable); ^{13}C NMR (100 MHz, DMSO-d_6, δ = ppm) δ = 13.77 (CH_3), 21.64 (CH_3), 103.87 (pyrazolopyrimidine C-3a), 121.98 (=CH), 127.22 (phenyl C-2, C-6), 127.50 (phenyl C-4), 128.83 (benzylidene C-4), 129.21 (*p*-tolyl C-1), 129.39 (benzylidene C-2, C-6), 129.71 (*p*-tolyl C-3, C-5), 129.94 (*p*-tolyl C-2, C-6), 131.26 (benzylidene C-3, C-5), 133.04 (phenyl C-3, C-5), 134.34 (triazine C-5), 135.86 (benzylidene C-1), 137.46 (*p*-tolyl C-4), 138.68 (phenyl C-1), 146.55 (pyrazolopyrimidine C-7a), 150.75 (pyrazolopyrimidine C-3), 155.69 (triazine C-3), 158.24 (pyrazolopyrimidine C-6), 160.11 (pyrazolopyrimidine C=O), 165.78 (triazine C=O), 168.37 (C=O); EIMS (*m/z*) 530 (M+1, 0.85%), 529 ($M^{+\cdot}$, 4.63%), 77 (100%). Anal.Calcd for $C_{30}H_{23}N_7O_3$(529.19): C, 68.04; H, 4.38; N, 18.52. Found: C, 68.13; H, 4.34; N, 18.49.

*4.1.1.5. (Z)-6-[5-(4-Methoxybenzylidene)-6-oxo-3-(p-tolyl)-1,2,5,6-tetrahydro-1,2,4-triazine-2-carbonyl]-3-methyl-1-phenyl-1H-pyrazolo[3,4-d]pyrimidin-4(5H)-one (**6e**).* Yellow solid; 56% yield; mp 380−382 °C; IR (KBr) 3198 (broad, 2NH), 3008 (CH-aromatic), 2924 (CH-aliphatic),1720-1675 (3C = O) cm^{-1}; ^1H NMR (400 MHz, DMSO-d_6, δ = ppm) δ = 2.35 (s, 3H, CH_3), 2.51 (s, 3H, CH_3), 3.86 (s, 3H, OCH_3), 7.11 (d, J = 8 Hz, 2H, *p*-methoxybenzylidene H-3, H-5), 7.30−7.40 (m, 3H, *p*-tolyl H-3, H-5 and = CH), 7.53−7.59 (m, 3H, phenyl H-3, H-4, H-5), 8.02 (d, J = 8 Hz, 2H, *p*-methoxybenzylidene H-2, H-6), 8.19 (d, J = 8 Hz, 2H, *p*-tolyl H-2, H-6), 8.36 (d, J = 8 Hz, 2H, phenyl H-2, H-6), 12.05 (s, 2H, 2NH, D_2O exchangeable); ^{13}C NMR (100 MHz, DMSO-d_6, δ = ppm) δ = 13.77 (CH_3), 21.52 (CH_3), 55.93 (OCH_3), 107.33 (pyrazolopyrimidine C-3a), 115.10 (*p*-methoxybenzylidene C-3, C-5), 121.94 (=CH), 124.92 (*p*-methoxybenzylidene C-1), 127.07 (phenyl C-2, C-6), 127.19 (*p*-tolyl C-1), 128.64 (phenyl C-4), 129.23 (*p*-tolyl C-3, C-5), 129.70 (*p*-tolyl C-2, C-6), 129.93 (*p*-methoxybenzylidene C-2, C-6), 134.42 (triazine C-5), 135.22 (phenyl C-3, C-5), 138.63 (*p*-tolyl C-4), 138.76 (phenyl C-1), 142.97 (pyrazolopyrimidine C-7a), 146.65 (pyrazolopyrimidine C-3), 151.56 (triazine C-3), 158.16 (pyrazolopyrimidine C-6), 158.77 (*p*-methoxybenzylidene C-4), 160.95 (pyrazolopyrimidine C=O), 162.03 (triazine C=O), 168.20 (C=O); Anal. Calcd for $C_{31}H_{25}N_7O_4$ (559.20): C, 66.54; H, 4.50; N, 17.52. Found: C, 66.57; H, 4.61; N, 17.58.

*4.1.1.6. (Z)-6-[5-(4-Chlorobenzylidene)-6-oxo-3-(p-tolyl)-1,2,5,6-tetrahydro-1,2,4-triazine-2-carbonyl]-3-methyl-1-phenyl-1H-pyrazolo[3,4-d]pyrimidin-4(5H)-one (**6f**).* Yellow solid; 54% yield; mp 378−380 °C; IR (KBr) 3368, 3194 (2NH), 3013 (CH-aromatic), 2928 (CH-aliphatic),1723-1678 (3C = O) cm^{-1}; ^1H NMR (400 MHz, DMSO-d_6, δ = ppm) δ = 2.35 (s, 3H, CH_3), 2.55 (s, 3H, CH_3), 7.21 (s, 1H,=CH), 7.55−7.60 (m, 7H, *p*-tolyl H-3, H-5, *p*-chlorobenzylidene H-3, H-5 and phenyl H-3, H-4, H-5), 8.09−8.11 (m, 4H, *p*-tolyl H-2, H-6 and *p*-chlorobenzylidene H-2, H-6), 8.30 (d, J = 8 Hz, 2H, phenyl H-2, H-6), 9.98 (s, 1H, NH, D_2O exchangeable), 11.10 (s, 1H, NH, D_2O exchangeable); ^{13}C NMR (100 MHz, DMSO-d_6, δ = ppm) δ = 14.00 (CH_3), 21.64 (CH_3), 104.56 (pyrazolopyrimidine C-3a), 121.91 (=CH), 127.19 (phenyl C-2, C-6), 128.96 (phenyl C-4), 129.50 (*p*-tolyl C-1), 129.71 (*p*-chlorobenzylidene C-3, C-5), 129.77 (*p*-chlorobenzylidene C-2, C-6), 130.15 (*p*-tolyl C-3, C-5), 131.11 (*p*-tolyl C-2, C-6), 132.43 (*p*-chlorobenzylidene C-1), 133.07 (*p*-chlorobenzylidene C-4), 134.40 (phenyl C-3, C-5), 135.46 (triazine C-5), 138.72 (phenyl C-1), 138.96 (*p*-tolyl C-4), 146.54 (pyrazolopyrimidine C-7a), 151.78 (pyrazolopyrimidine C-3), 154.84 (triazine C-3), 158.77 (pyrazolopyrimidine C-6), 160.08 (pyrazolopyrimidine C=O), 163.14 (triazine C=O), 168.51 (C=O); Anal. Calcd for $C_{30}H_{22}ClN_7O_3$ (563.15): C, 63.89; H, 3.93; N, 17.38. Found: C, 63.92; H, 3.87; N, 17.35.

*4.1.1.7. (Z)-6-(5-Benzylidene-3(4-chlorophenyl)-6-oxo-1,2,5,6-tetrahydro-1,2,4-triazine-2-carbonyl)-3-methyl-1-phenyl-1H-pyrazolo[3,4-d]pyrimidin-4(5H)-one (**6g**).* Yellow solid; 31% yield; mp 297−299 °C; IR (KBr) 3217, 3132 (2NH), 3032 (CH-aromatic), 2928 (CH-aliphatic),1720-1673 (3C = O) cm^{-1}; ^1H NMR (400 MHz, DMSO-d_6, δ = ppm) δ = 2.58 (s, 3H, CH_3), 7.39−7.45 (m, 3H, = CH and *p*-chlorophenyl H-2, H-6), 7.53−7.66 (m, 6H, benzylidene H-3, H-4, H-5 and phenyl H-3, H-4, H-5), 8.12 (d, J = 7.6 Hz, 2H, benzylidene H-2,H-6), 8.23 (d, J = 8.4 Hz, 2H, phenyl H-2, H-6), 8.41 (d, J = 8.4 Hz, 2H, *p*-chlorophenyl H-3, H-5), 12.09 (s, 1H, NH, D_2O exchangeable), 12.70 (s, 1H, NH, D_2O exchangeable); ^{13}C NMR (100 MHz, DMSO-d_6, δ = ppm) δ = 13.74 (CH_3), 107.41 (pyrazolopyrimidine C-3a), 121.89 (=CH), 127.22 (*p*-chlorophenyl C-1), 127.25 (phenyl C-2, C-6), 128.31 (benzylidene C-4), 128.88 (benzylidene C-3, C-5), 129.46 (benzylidene C-2, C-6), 129.56 (*p*-chlorophenyl C-2, C-6), 129.79 (*p*-chlorophenyl C-3, C-5), 133.06 (triazine

C-5), 133.20 (phenyl C-4), 134.73 (phenyl C-3, C-5), 136.17 (benzylidene C-1), 136.52 (*p*-chlorophenyl C-4), 138.52 (phenyl C-1), 146.83 (pyrazolopyrimidine C-7a), 147.43 (pyrazolopyrimidine C-3), 151.20 (triazine C-3), 158.08 (pyrazolopyrimidine C-6), 159.07(pyrazolopyrimidine C=O), 160.45 (triazine C=O), 168.04 (C=O); Anal. Calcd for $C_{29}H_{20}ClN_7O_3$ (549.13): C, 63.33; H, 3.67; N, 17.83. Found: C, 63.21; H, 3.54; N, 17.81.

*4.1.1.8. (Z)-6-[3-(4-Chlorophenyl)-5-(4-methoxybenzylidene)-6-oxo-1,2,5,6-tetrahydro-1,2,4-triazine-2-carbonyl]-3-methyl-1-phenyl-1H-pyrazolo[3,4-d]pyrimidin-4(5H)-one (**6h**).* Yellow solid; 59% yield; mp 335–337 °C; IR (KBr) 3294, 3132 (2NH), 3048 (CH-aromatic), 2928 (CH-aliphatic),1722-1679 (3C = O) cm^{-1}; ^1H NMR (400 MHz, DMSO-d_6, δ = ppm) δ = 2.56 (s, 3H, CH_3), 3.86 (s, 3H, OCH_3), 7.11 (d, *J* = 7.4 Hz, 2H, *p*-methoxybenzylidene H-3, H-5), 7.32 (s, 1H, = CH), 7.53–7.60 (m, 5H, *p*-chlorophenyl H-2, H-6 and phenyl H-3, H-4, H-5), 8.13 (d, *J* = 7.4 Hz, 2H, *p*-methoxybenzylidene H-2,H-6), 8.22 (d, *J* = 8 Hz, 2H, phenyl H-2, H-6), 8.36 (d, *J* = 8.8 Hz, 2H, *p*-chlorophenyl H-3, H-5), 12.02 (s, 1H, NH, D_2O exchangeable), 12.06 (s, 1H, NH, D_2O exchangeable); ^{13}C NMR (100 MHz, DMSO-d_6, δ = ppm) δ = 13.78 (CH_3), 55.95 (OCH_3), 107.17 (pyrazolopyrimidine C-3a), 115.13 (*p*-methoxybenzylidene C-3, C-5), 121.46 (=CH), 121.98 (phenyl C-2, C-6), 126.67 (*p*-methoxybenzylidene C-1), 127.19 (phenyl C-4), 129.46 (*p*-chlorophenyl C-3, C-5), 129.63 (*p*-chlorophenyl C-2, C-6), 130.44 (*p*-methoxybenzylidene C-2, C-6), 132.20 (*p*-chlorophenyl C-1), 134.03 (triazine C-5), 135.30 (phenyl C-3, C-5), 137.38 (*p*-chlorophenyl C-4), 146.21 (phenyl C-1), 148.91 (pyrazolopyrimidine C-7a), 152.42 (pyrazolopyrimidine C-3), 156.22 (triazine C-3), 157.81 (pyrazolopyrimidine C-6), 160.58 (*p*-methoxybenzylidene C-4), 162.12 (pyrazolopyrimidine C=O), 166.28 (triazine C=O), 168.10 (C=O); Anal. Calcd for $C_{30}H_{22}ClN_7O_4$ (579.14): C, 62.13; H, 3.82; N, 16.90. Found: C, 62.27; H, 3.75; N, 17.11.

*4.1.1.9. (Z)-6-[5-(4-Chlorobenzylidene)-3-(4-chlorophenyl)-6-oxo-1,2,5,6-tetrahydro-1,2,4-triazine-2-carbonyl]-3-methyl-1-phenyl-1H-pyrazolo[3,4-d]pyrimidin-4(5H)-one (**6i**).* Yellow solid; 43% yield; mp 292–294 °C; IR (KBr) 3395, 3194 (2NH), 3021 (CH-aromatic), 2940 (CH-aliphatic),1724-1670 (3C = O) cm^{-1}; ^1H NMR (400 MHz, DMSO-d_6, δ = ppm) δ = 2.50 (s, 3H, CH_3), 7.07–7.12 (m, 4H, *p*-chlorobenzylidene H-3, H-5 and *p*-chlorophenyl H-2, H-6), 7.23 (s, 1H, =CH), 7.37 (t, *J* = 7.2 Hz, 1H, phenyl H-4), 7.53 (t, *J* = 8 Hz, 2H, phenyl H-3, H-5), 7.84 (d, *J* = 8.4 Hz, 2H, *p*-chlorobenzylidene H-2, H-6), 8.05 (d, *J* = 8 Hz, 2H, phenyl H-2, H-6), 8.32 (d, *J* = 8.8 Hz, 2H, *p*-chlorophenyl H-3, H-5), 11.36 (s, 1H, NH, D_2O exchangeable), 12.45 (s, 1H, NH, D_2O exchangeable); ^{13}C NMR (100 MHz, DMSO-d_6, δ = ppm) δ = 13.77 (CH_3), 104.73 (pyrazolopyrimidine C-3a), 115.06 (phenyl C-2, C-6), 121.68(=CH), 124.87 (*p*-chlorophenyl C-1), 126.91 (phenyl C-4), 127.08 (*p*-chlorobenzylidene C-1), 128.39 (*p*-chlorobenzylidene C-3, C-5), 128.91 (*p*-chlorophenyl C-3, C-5), 129.59 (*p*-chlorobenzylidene C-2, C-6), 129.66 (*p*-chlorophenyl C-2, C-6), 134.33 (triazine C-5), 135.13 (phenyl C-3, C-5), 138.79 (*p*-chlorobenzylidene C-4), 142.70 (*p*-chlorophenyl C-4), 146.29 (phenyl C-1), 152.86 (pyrazolopyrimidine C-7a), 155.20 (pyrazolopyrimidine C-3), 158.70 (triazine C-3), 158.86 (pyrazolopyrimidine C-6), 161.94 (pyrazolopyrimidine C=O), 166.28 (triazine C=O), 168.32 (C=O); EIMS (*m/z*) 583 ($M^{+\cdot}$, 1.12%), 91 (100%). Anal.Calcd for $C_{29}H_{19}Cl_2N_7O_3$ (583.09): C, 59.60; H, 3.28; N, 16.78. Found: C, 59.58; H, 3.14; N, 16.88.

*4.1.1.10. (E)-6-[2-(5-Benzylidene-6-oxo-3-phenyl-5,6-dihydro-1,2,4-triazine-2(1H)-yl)-2-oxoethyl]-3-methyl-1-phenyl-1H-pyrazolo[3,4-d]pyrimidin-4(5H)-one (**6j**).* Yellow solid; 43% yield; mp 242–244 °C; IR (KBr) 3294, 3148 (2NH), 3067 (CH-aromatic), 2994-2924 (CH-aliphatic), 1721-1668 (3C = O) cm^{-1}; ^1H NMR (400 MHz, DMSO-d_6, δ = ppm) δ = 2.52 (s, 3H, CH_3), 4.09 (s, 2H, CH_2), 7.36 (s, 1H, =CH), 7.52 (t, *J* = 7.6 Hz, 1H, benzylidene H-4), 7.57–7.68 (m, 5H, phenyl H-3, H-4, H-5 and benzylidene H-3 and H-5), 7.75 (t, *J* = 7.6 Hz, 1H, pyrazolopyrimidine phenyl H-4), 7.96 (d, *J* = 8 Hz, 2H, benzylidene H-2, H-6), 8.03 (d, *J* = 8 Hz, 2H, phenyl H-2, H-6), 8.15 (d, *J* = 8 Hz, 2H, pyrazolopyrimidine phenyl H-3, H-5), 8.35 (d, *J* = 8 Hz, 2H, pyrazolopyrimidine phenyl H-2, H-6),11.41 (s, 1H, NH, D_2O exchangeable), 12.45 (s, 1H, NH, D_2O exchangeable); ^{13}C NMR (100 MHz, DMSO-d_6, δ = ppm) δ = 13.76 (CH_3), 49.07 (CH_2), 104.75 (pyrazolopyrimidine C-3a), 121.82 (=CH), 125.47 (pyrazolopyrimidine phenyl C-2, C-6),127.08 (pyrazolopyrimidine phenyl C-4), 127.86 (benzylidene C-4), 128.16 (phenyl C-2, C-6), 128.57 (phenyl C-3, C-5), 128.66 (benzylidene C-2, C-6), 128.72 (benzylidene C-3, C-5), 128.98 (phenyl C-4), 131.82 (phenyl C-1), 132.84 (triazine C-5), 133.10 (pyrazolopyrimidine phenyl C-3, C-5), 134.59 (benzylidene C-1), 139.72 (pyrazolopyrimidine phenyl C-1), 146.48 (pyrazolopyrimidine C-7a), 152.83 (pyrazolopyrimidine C-3), 155.13 (triazine C-3), 158.83 (pyrazolopyrimidine C-6), 163.89 (pyrazolopyrimidine C=O), 166.44 (triazine C=O), 167.26 (C=O); Anal. Calcd for $C_{30}H_{23}N_7O_3$ (529.19): C, 68.04; H, 4.38; N, 18.52. Found: C, 68.13; H, 4.24; N, 18.56.

*4.1.1.11. (E)-6-{2-[5-(4-Methoxybenzylidene)-6-oxo-3-phenyl-5,6-dihydro-1,2,4-triazine-2(1H)-yl]-2-oxoethyl}-3-methyl-1-phenyl-1H-pyrazolo[3,4-d]pyrimidin-4(5H)-one (**6k**).* Yellow solid; 32% yield; mp 277–279 °C; IR (KBr) 3198 (broad, 2NH), 3009 (CH-aromatic), 2928 (CH-aliphatic), 1720-1680 (3C = O) cm^{-1}; ^1H NMR (400 MHz, DMSO-d_6, δ = ppm) δ = 2.52 (s, 3H, CH_3), 3.68 (s, 2H, CH_2), 3.84 (s, 3H, OCH_3), 7.08 (d, *J* = 8.2 Hz, 2H, *p*-methoxybenzylidene H-3, H-5), 7.26 (s, 1H, =CH), 7.35–7.38 (m, 4H, phenyl H-3, H-4, H-5, pyrazolopyrimidine phenyl H-4), 7.48–7.55 (m, 4H, *p*-methoxybenzylidene H-2, H-6, pyrazolopyrimidine phenyl H-3, H-5), 7.94 (d, *J* = 7.2 Hz, 2H, phenyl H-2, H-6), 8.33 (d, *J* = 8.8 Hz, 2H, pyrazolopyrimidine phenyl H-2, H-6), 10.11 (s, 1H, NH, D_2O exchangeable), 12.33 (s, 1H, NH, D_2O exchangeable);^{13}C NMR (100 MHz, DMSO-d_6, δ = ppm) δ = 13.77 (pyrazolopyrimidine CH_3), 40.59 (CH_2), 55.92 (OCH_3), 104.59 (pyrazolopyrimidine C-3a), 115.08 (*p*-methoxybenzylidene C-3, C-5), 121.71 (=CH), 126.93 (pyrazolopyrimidine phenyl C-2, C-6), 126.99 (*p*-methoxybenzylidene C-1), 127.05 (phenyl C-2, C-6), 127.71 (pyrazolopyrimidine phenyl C-4), 128.44 (phenyl C-3, C-5), 129.10 (phenyl C-4), 129.48 (*p*-methoxybenzylidene C-2, C-6), 132.38 (phenyl C-1), 134.28 (pyrazolopyrimidine C-3, C-5), 135.23 (triazine C-5), 138.78 (pyrazolopyrimidine phenyl C-1), 146.28 (pyrazolopyrimidine C-7a), 152.86 (pyrazolopyrimidine C-3), 155.21 (triazine C-3), 156.34 (pyrazolopyrimidine C-6), 158.85 (*p*-methoxybenzylidene C-4), 165.83 (pyrazolopyrimidine C=O), 166.42 (triazine C=O), 168.24 (C=O); Anal. Calcd for $C_{31}H_{25}N_7O_4$ (559.20): C, 66.54; H, 4.50; N, 17.52. Found: C, 66.48; H, 4.61; N, 17.57.

*4.1.1.12. (E)-6-{2-[5-(4-Chlorobenzylidene)-6-oxo-3-phenyl-5,6-dihydro-1,2,4-triazine-2(1H)-yl]-2-oxoethyl}-3-methyl-1-phenyl-1H-pyrazolo[3,4-d]pyrimidin-4(5H)-one (**6l**).* Yellow solid; 33% yield; mp 310–312 °C; IR (KBr) 3229, 3198 (2NH), 3009 (CH-aromatic), 2947 (CH-aliphatic), 1716-1674 (3C = O) cm^{-1}; ^1H NMR (400 MHz, DMSO-d_6, δ = ppm) δ = 2.73 (s, 3H, CH_3), 3.94 (s, 2H, CH_2), 7.32 (s, 1H, =CH), 7.36–7.40 (m, 3H, phenyl H-3, H-4, H-5), 7.52–7.56 (m, 3H, pyrazolopyrimidine phenyl H-3, H-4, H-5), 7.57 (d, *J* = 7.6 Hz, 2H, phenyl H-2, H-6), 7.97 (d, *J* = 7.6 Hz, 2H, pyrazolopyrimidine phenyl H-2, H-6), 8.03 (d, *J* = 8 Hz, 2H, *p*-chlorophenyl H-3, H-5), 8.36 (d, *J* = 8 Hz, 2H, *p*-chlorophenyl H-2, H-6), 11.41 (s, 1H, NH, D_2O exchangeable), 12.45 (s, 1H, NH, D_2O exchangeable); ^{13}C NMR (100 MHz, DMSO-d_6, δ = ppm) δ = 13.76 (CH_3), 49.06 (CH_2), 104.70 (pyrazolopyrimidine C-3a), 121.81 (=CH), 127.07 (pyrazolopyrimidine phenyl C-2, C-6), 127.36 (phenyl C-1), 127.67 (pyrazolopyrimidine phenyl C-4), 128.66 (phenyl C-2, C-6), 129.16 (*p*-

chlorophenyl C-3, C-5), 129.50 (phenyl C-3, C-5), 129.64 (*p*-chlorophenyl C-2, C-6), 133.83 (*p*-chlorophenyl C-1), 133.12 (phenyl C-4), 134.60 (pyrazolopyrimidine phenyl C-3, C-5), 135.96 (*p*-chlorophenyl C-4), 136.66 (triazine C-5), 138.75 (pyrazolopyrimidine phenyl C-1), 146.33 (pyrazolopyrimidine C-7a), 152.84 (pyrazolopyrimidine C-3), 155.15 (triazine C-3), 158.81 (pyrazolopyrimidine C-6), 160.75 (pyrazolopyrimidine C=O), 166.43 (triazine C=O), 168.25 (C=O); EIMS (*m/z*) 564 ($M^{+\cdot}$, 15.75%), 129 (100%). Anal.Calcd for $C_{30}H_{22}ClN_7O_3$ (563.15): C, 63.89; H, 3.93; N, 17.38. Found: C, 63.78; H, 4.01; N, 17.27.

*4.1.1.13. (E)-6-[2-(5-Benzylidene-6-oxo-3-(p-tolyl)-5,6-dihydro-1,2,4-triazine-2(1H)-yl)-2-oxoethyl]-3-methyl-1-phenyl-1H-pyrazolo[3,4-d]pyrimidin-4(5H)-one (**6m**).* Buff solid; 32% yield; mp 294–296 °C; IR (KBr) 3275, 3125 (2NH), 3009 (CH-aromatic), 2986, 2924 (CH-aliphatic),1715-1668 (3C = O) cm^{-1}; ^1H NMR (400 MHz, DMSO-d_6, δ = ppm) δ = 2.34 (s, 3H, CH_3), 2.54 (s, 3H, CH_3), 3.68 (s, 2H, CH_2), 7.15 (d, *J* = 7.6 Hz, *p*-tolyl H-3, H-5), 7.24 (s, 1H, =CH), 7.48–7.56 (m,4H, phenyl H-4, benzylidene H-3, H-4, H-5), 7.79 (t, *J* = 8 Hz, 2H, phenyl H-3, H-5), 8.02 (d, *J* = 8.2 Hz, 2H, benzylidene H-2, H-6), 8.17 (d, *J* = 7.6 Hz, 2H, *p*-tolyl H-2, H-6), 8.25 (d, *J* = 7.4 Hz, 2H, phenyl H-2, H-6), 9.81 (s, 1H, NH, D_2O exchangeable), 12.03 (s, 1H, NH, D_2O exchangeable); ^{13}C NMR (100 MHz, DMSO-d_6, δ = ppm) δ = 13.95 (CH_3), 22.63 (CH_3), 39.90 (CH_2), 106.06 (pyrazolopyrimidine C-3a), 120.52 (=CH), 121.28 (phenyl C-2, C-6), 121.83 (phenyl C-4), 125.43 (benzylidene C-2, C-6), 126.30 (benzylidene C-3, C-5), 127.08 (benzylidene C-4), 127.97 (*p*-tolylC-3, C-5), 128.58 (*p*-tolyl C-2, C-6), 129.43 (*p*-tolyl C-1), 129.59 (phenyl C-3, C-5), 134.75 (phenyl C-1), 136.71 (triazine C-5), 137.81 (benzylidene C-1), 139.41 (*p*-tolyl C-4), 146.05 (pyrazolopyrimidine C-7a), 149.69 (pyrazolopyrimidine C-3), 154.31 (triazine C-3), 155.71 (pyrazolopyrimidine C-6), 161.39 (pyrazolopyrimidine C=O), 164.67 (triazine C=O), 168.60 (C=O); Anal. Calcd for $C_{31}H_{25}N_7O_3$ (543.20): C, 68.50; H, 4.64; N, 18.04. Found: C, 68.37; H, 4.71; N, 17.98.

*4.1.1.14. (E)-6-[2-(5-(4-Methoxybenzylidene)-6-oxo-3-(p-tolyl)-5,6-dihydro-1,2,4-triazine-2(1H)-yl)-2-oxoethyl]-3-methyl-1-phenyl-1H-pyrazolo[3,4-d]pyrimidin-4(5H)-one (**6n**).* Yellow solid; 57% yield; mp 311–313 °C; IR (KBr) 3368, 3194 (2NH), 3021 (CH-aromatic), 2943 (CH-aliphatic), 1724-1670 (3C = O) cm^{-1}; ^1H NMR (400 MHz, DMSO-d_6, δ = ppm) δ = 2.25 (s, 3H, CH_3), 2.53 (s, 3H, CH_3), 3.68 (s, 3H, OCH_3), 3.85 (s, 2H, CH_2), 7.07–7.12 (m, 4H, *p*-tolyl H-3, H-5 and *p*-methoxybenzylidene H-3, H-5), 7.23 (s, 1H, =CH), 7.38 (t, *J* = 7.6 Hz, 1H, phenyl H-4), 7.53 (d, *J* = 7.6 Hz, 2H, phenyl H-3, H-5), 7.84 (d, *J* = 8 Hz, 2H, *p*-methoxybenzylidene H-2, H-6), 8.05 (d, *J* = 8.4 Hz, 2H, phenyl H-2, H-6), 8.31 (d, *J* = 8.8 Hz, 2H, *p*-tolyl H-2, H-6), 11.35 (s, 1H, NH, D_2O exchangeable), 12.45 (s, 1H, NH, D_2O exchangeable); ^{13}C NMR (100 MHz, DMSO-d_6, δ = ppm) δ = 13.77 (CH_3), 21.52 (CH_3), 39.97 (CH_2), 55.93 (OCH_3), 107.33 (pyrazolopyrimidine C-3a), 115.10 (*p*-methoxybenzylidene C-3, C-5), 121.71 (=CH), 121.94 (phenyl C-2, C-6), 124.92 (*p*-methoxybenzylidene C-1), 127.07 (*p*-tolyl C-1), 127.19 (*p*-methoxybenzylidene C-2, C-6), 128.64 (phenyl C-4), 129.23 (*p*-tolyl C-3, C-5), 129.70 (*p*-tolyl C-2, C-6), 129.93 (phenyl C-1), 134.42 (phenyl C-3, C-5), 135.22 (triazine C-5), 138.63 (*p*-tolyl C-4), 138.76 (pyrazolopyrimidine C-7a), 142.97 (pyrazolopyrimidine C-3), 146.65 (triazine C-3), 158.16 (pyrazolopyrimidine C-6), 158.77 (*p*-methoxybenzylidene C-4), 160.09 (pyrazolopyrimidine C=O), 162.03 (triazine C=O), 168.20 (C=O); EIMS (*m/z*) 574 (M+1, 7.17%), 573 ($M^{+\cdot}$, 10.14%), 77 (100%). Anal.Calcd for $C_{32}H_{27}N_7O_4$ (573.21): C, 67.01; H, 4.74; N, 17.09. Found: C, 67.13; H, 4.65; N, 17.11.

*4.1.1.15. (E)-6-[2-(5-(4-Chlorobenzylidene)-6-oxo-3-(p-tolyl)-5,6-dihydro-1,2,4-triazine-2(1H)-yl)-2-oxoethyl]-3-methyl-1-phenyl-1H-pyrazolo[3,4-d]pyrimidin-4(5H)-one (**6o**).* Yellow solid; 42% yield; mp 308–310 °C; IR (KBr) 3368, 3194 (2NH), 3021 (CH-aromatic), 2943 (CH-aliphatic),1724-1689 (3C = O) cm^{-1}; ^1H NMR (400 MHz, DMSO-d_6, δ = ppm) δ = 2.26 (s, 3H, CH_3), 2.53 (s, 3H, CH_3), 3.80 (s, 2H, CH_2), 7.12 (d, *J* = 8 Hz, 2H, *p*-tolyl H-3, H-5), 7.27 (s, 1H, =CH), 7.38 (t, *J* = 8 Hz, 1H, phenyl H-4), 7.52 (t, *J* = 8 Hz, 2H, phenyl H-3, H-5), 7.58 (d, *J* = 8.4 Hz, 2H, *p*-chlorophenyl H-3, H-5), 7.86 (d, *J* = 8 Hz, 2H, *p*-tolyl H-2, H-6), 8.05 (d, *J* = 8 Hz, 2H, phenyl H-2, H-6), 8.35 (d, *J* = 8.4 Hz, 2H, *p*-chlorophenyl H-2, H-6), 11.41 (s, 1H, NH, D_2O exchangeable), 12.24 (s, 1H, NH, D_2O exchangeable); ^{13}C NMR (100 MHz, DMSO-d_6, δ = ppm) δ = 13.78 (CH_3), 21.60 (CH_3), 39.99 (CH_2), 104.74 (pyrazolopyrimidine C-3a), 121.66 (=CH), 124.54 (*p*-tolyl C-1), 127.00 (phenyl C-2, C-6), 127.05 (phenyl C-4), 128.62 (*p*-chlorophenyl C-3, C-5), 129.48 (*p*-chlorophenyl C-2, C-6), 129.62 (*p*-tolyl C-3, C-5), 129.73 (*p*-tolyl C-2, C-6), 133.22 (*p*-chlorophenyl C-1), 134.51 (phenyl C-3, C-5), 135.80 (*p*-chlorophenyl C-4), 136.72 (triazine C-5), 138.80 (phenyl C-1), 143.25 (*p*-tolyl C-4), 146.33 (pyrazolopyrimidine C-7a), 152.85 (pyrazolopyrimidine C-3), 155.16 (triazine C-3), 158.80 (pyrazolopyrimidine C-6), 160.59 (pyrazolopyrimidine C=O), 166.27 (triazine C=O), 168.32 (C=O); Anal. Calcd for $C_{31}H_{24}ClN_7O_3$ (577.16): C, 64.41; H, 4.19; N, 16.96. Found: C, 64.37; H, 4.15; N, 17.11.

*4.1.1.16. (E)-6-[2-(5-(4-Benzylidene)-3-(4-chlorophenyl)-6-oxo-5,6-dihydro-1,2,4-triazine-2(1H)-yl)-2-oxoethyl]-3-methyl-1-phenyl-1H-pyrazolo[3,4-d]pyrimidin-4(5H)-one (**p**).* Buff solid; 48% yield; mp 291–293 °C; IR (KBr) 3294, 3148 (2NH), 3067 (CH-aromatic), 2994, 2928 (CH-aliphatic),1720-1668 (3C = O) cm^{-1}; ^1H NMR (400 MHz, DMSO-d_6, δ = ppm) δ = 2.47 (s, 3H, CH_3), 3.61 (s, 2H, CH_2), 7.22 (s, 1H, =CH), 7.33 (t, *J* = 7.8 Hz, 1H, benzylidene H-4), 7.39 (d, *J* = 8 Hz, 2H, *p*-chlorophenyl H-2, H-6), 7.40 (t, *J* = 7.8 Hz, 2H, benzylidene H-3, H-5), 7.45 (t, *J* = 7.2 Hz, 1H, phenyl H-4), 7.52 (d, *J* = 8 Hz, 2H, *p*-chlorophenyl H-3, H-5), 7.58 (t, *J* = 7.2 Hz, 2H, phenyl H-3, H-5), 7.60 (d, *J* = 7.2 Hz, 2H, benzylidene H-2, H-6), 8.04 (d, *J* = 7.6 Hz, 2H, phenyl H-2, H-6), 11.37 (s, 1H, NH, D_2O exchangeable), 12.26 (s, 1H, NH, D_2O exchangeable); ^{13}C NMR (100 MHz, DMSO-d_6, δ = ppm) δ = 13.40 (CH_3), 38.19 (CH_2), 105.34 (pyrazolopyrimidine C-3a), 121.66 (=CH), 123.90 (phenyl C-2, C-6), 126.25 (phenyl C-4), 127.93 (benzylidene C-4), 128.50 (benzylidene C-2, C-6), 128.61 (benzylidene C-3, C-5), 128.92 (*p*-chlorophenyl C-3, C-5), 129.18 (*p*-chlorophenyl C-2, C-6), 129.32 (phenyl C-3, C-5), 130.4 (*p*-chlorophenyl C-1), 134.5 (triazine C-5), 135.20 (phenyl of triazine C-1), 135.76 (*p*-chlorophenyl C-4), 139.73 (phenyl C-1), 144.43 (pyrazolopyrimidine C-7a), 149.25 (pyrazolopyrimidine C-3), 156.26 (triazine C-3), 158.40 (pyrazolopyrimidine C-6), 160.89 (pyrazolopyrimidine C=O), 165.87 (triazine C=O), 168.62 (C=O); Anal.Calcd for $C_{30}H_{22}ClN_7O_3$ (563.15): C, 63.89; H, 3.93; N, 17.38. Found: C, 63.77; H, 4.07; N, 17.43.

*4.1.1.17. (E)-6-[2-(3-(4-Chlorophenyl)-5-(4-methoxybenzylidene)-6-oxo-5,6-dihydro-1,2,4-triazine-2(1H)-yl)-2-oxoethyl]-3-methyl-1-phenyl-1H-pyrazolo[3,4-d]pyrimidin-4(5H)-one (**q**).* Yellow solid; 52% yield; mp299-301 °C; IR (KBr) 3368, 3190 (2NH), 3071 (CH-aromatic), 2936 (CH-aliphatic),1724-1670 (3C = O) cm^{-1}; ^1H NMR (400 MHz, DMSO-d_6, δ = ppm) δ = 2.53 (s, 3H, CH_3), 3.81 (s, 2H, CH_2), 3.85 (s, 3H, OCH_3), 7.09 (d, *J* = 8.4 Hz, 2H, *p*-methoxybenzylidene H-3, H-5), 7.29 (s, 1H, =CH), 7.38–7.40 (m, 3H, phenyl H-4 and *p*-chlorophenyl H-3, H-5), 7.53 (t, *J* = 8 Hz, 2H, phenyl H-3, H-5), 7.95 (d, *J* = 8.4 Hz, 2H, *p*-methoxybenzylidene H-2, H-6), 8.04 (d, *J* = 7.6 Hz, 2H, phenyl H-2, H-6), 8.32 (d, *J* = 8.8 Hz, 2H, *p*-chlorophenyl H-2, H-6), 11.37 (s, 1H, NH, D_2O exchangeable), 12.45 (s, 1H, NH, D_2O exchangeable);^{13}C NMR (100 MHz, DMSO-d_6, δ = ppm) δ = 13.77 (CH_3), 40.59 (CH_2), 55.94 (OCH_3), 104.72 (pyrazolopyrimidine C-3a), 115.12 (*p*-methoxybenzylidene C-3, C-5), 121.69 (=CH), 126.48 (*p*-chlorophenyl C-1), 126.94 (*p*-methoxybenzylidene C-1), 127.06 (phenyl C-2, C-6), 129.29 (*p*-chlorophenyl

C-3, C-5), 129.64 (*p*-chlorophenyl C-2, C-6), 129.96 (phenyl C-4), 130.15 (*p*-methoxybenzylidene C-2, C-6), 134.10 (triazine C-5), 135.32 (phenyl C-3, C-5), 137.38 (*p*-chlorophenyl C-4), 138.75 (phenyl C-1), 146.34 (pyrazolopyrimidine C-7a), 152.82 (pyrazolopyrimidine C-3), 155.17 (triazine C-3), 157.82 (pyrazolopyrimidine C-6), 158.81 (*p*-methoxybenzylidene C-4), 162.16 (pyrazolopyrimidine C=O), 166.46 (triazineC = O), 168.11(C=O); EIMS (*m/z*) 595 (M+2, 0.91%), 593 (M + ., 2.16%), 57 (100%). Anal.Calcd for $C_{31}H_{24}ClN_7O_4$ (593.16): C, 62.68; H, 4.07; N, 16.51. Found: C, 62.59; H, 4.13; N, 16.55.

*4.1.1.18. (E)-6-[2-(5-(4-Chlorobenzylidene)-3-(4-chlorophenyl)-6-oxo-5,6-dihydro-1,2,4-triazine-2(1H)-yl)-2-oxoethyl]-3-methyl-1-phenyl-1H-pyrazolo[3,4-d]pyrimidin-4(5H)-one (**r**).* Yellow solid; 55% yield; mp314-316 °C; IR (KBr) 3213 (broad, 2NH), 3071 (CH-aromatic), 2932 (CH-aliphatic),1724-1667 (3C = O) cm^{-1}; ^1H NMR (400 MHz, DMSO-d_6, δ = ppm) δ = 2.53 (s, 3H, CH_3), 3.81 (s, 2H, CH_2), 7.34 (s, 1H, =CH), 7.37−7.42 (m, 3H, phenyl H-4, *p*-chlorophenyl H-2, H-6), 7.53 (t, *J* = 8.4 Hz, 2H, phenyl H-3, H-5), 7.58 (d, *J* = 8.8 Hz, 2H, *p*-chlorobenzylidene H-3, H-5), 7.97 (d, *J* = 8.8 Hz, 2H, *p*-chlorophenyl H-3, H-5), 8.05 (d, *J* = 8.8 Hz, 2H, *p*-chlorobenzylidene H-2, H-6), 8.35 (d, *J* = 8.4 Hz, 2H, phenyl H-2, H-6), 11.43 (s, 1H, NH, D_2O exchangeable), 12.44 (s, 1H, NH, D_2O exchangeable);^{13}C NMR (100 MHz, DMSO-d_6, δ = ppm) δ = 13.77 (pyrazolopyrimidine CH_3), 40.56 (CH_2), 104.71 (pyrazolopyrimidine C-3a), 121.69 (=CH), 126.12 (*p*-chlorophenyl C-1), 127.08 (phenyl C-2, C-6), 128.13 (phenyl C-4), 129.35 (*p*-chlorobenzylidene C-3, C-5), 129.52 (*p*-chlorophenyl C-3, C-5), 129.64 (*p*-chlorobenzylidene C-2, C-6), 130.39 (*p*-chlorophenyl C-2, C-6), 133.03 (*p*-chlorobenzylidene C-1), 134.65 (phenyl C-3, C-5), 136.11 (*p*-chlorobenzylidene C-4), 136.48 (triazine C-5), 137.87 (phenyl C-1), 138.73 (*p*-chlorophenyl C-4), 146.35 (pyrazolopyrimidine C-7a), 152.81 (pyrazolopyrimidine C-3), 155.11 (triazine C-3), 158.82 (pyrazolopyrimidine C-6), 159.77 (pyrazolopyrimidine C=O), 166.47 (triazine C=O), 168.13 (C=O); Anal.Calcd for $C_{30}H_{21}Cl_2N_7O_3$ (597.11): C, 60.21; H, 3.54; N, 16.38. Found: C, 60.11; H, 3.60; N, 16.43.

4.2. Biological evaluation

4.2.1. Measurment of cytotoxic activity

4.2.1.1. Materials and methods. In this research, breast adenocarcinoma (MCF-7), colon carcinoma (HCT-116) and human fibroblast (WI38) cell lines were obtained from American Type Culture Collection (ATCC) and maintained at VACSERA, Giza, Egypt. Lapatinib was used as a reference drug. Cells were cultured in Dulbecco's Modified Eagle's medium (DMEM) (Invitrogen/Life Technologies) supplemented with 10% FBS (Hyclone), 10 μg/ml of insulin (Sigma), and 1% penicillin-streptomycin. Sigma or Invitrogen was used as a source for all of the other chemicals and reagents.

Before the MTT assay, plate cells were maintained (cells density 1.2−1.8 × 10,000 cells/well) in a volume of 100 μl complete growth medium + 100 μl of the tested compound per well in a 96-well plate for 24 h.

4.2.1.2. Cytotoxic activity using MTT assay. MTT [3-(4,5-dimrthylthiazol-2-yl)-2,5-diphenyltetrazolium bromide] assay was used to measure the cytotoxic activity for the tested compounds and the reference drug according to the described method [32]. For best results, cells were plated in 96-multiwell plate in DMEM containing 10% FBS (fetal bovine serum) for 24 h. Then, cells, test compounds and reference drug were treated with vehicle DMSO for 48 h. After that, the media was replaced with 200 μl DMEM containing 0.5 mg/ml of MTT and were incubated for 2 h. After the incubation period, dissolve the resulting formazan crystals using 200 μL of DMSO. Spectrophotometrically measure absorbance at a wave length 570 nm using a micro plate reader [38].

4.2.2. Cell cycle analysis using DNA-flow cytometry

Both HCT-116 and MCF-7 cells were treated with compounds **6o** and **6q**, respectively, at their IC_{50} values and incubated for 24 h. After incubation, the cells were washed with cold phosphate buffered saline (PBS) and fixed with 70% ethanol. The fixed cells were rinsed with PBS and then stained with propidium iodide (PI) in a solution containing Triton X-100 as well as RNase, keep 15 min at 37 °C according the instruction manual. Then the samples were analyzed with a FACS Caliber flow cytometer (Becton Dickinson & Co., Franklin Lakes, NJ) [38].

4.2.3. Measurement of apoptosis using Annexin-V-FITC/PIstaining

To assess apoptosis and necrosis using Annexin V-FITC/PI apoptosis detection kit, the cells were stained with Annexin V-fluorescein isothiocyanate (FITC) and counterstaining with propidium iodide (PI). 2 × 10^5 Cells were exposed to compounds **6o** and **6q** at IC_{50} values (4.8 and 6.5 nM) for 24 h and 48 h. Then, the cells were trypsinized and washed in cold phosphate-buffered saline (PBS), stained with Annexin V-FITC and PI for 15 min at 37 °C in the dark. Finally, the samples were analyzed using flow cytometer (FACS Caliber, Becton Dickinson Biosciences & Co., Franklin Lakes, NJ). For each sample, the number of analyzed cells was 10000 [38].

4.2.4. Measurment of apoptotic biomarkers using ELISA immunoassay technique

4.2.4.1. Measurement of human active caspase-3/7/9, Bax and Bcl2 content. To allow cells of HCT-116 and MCF-7 that obtained from ATCC to grow at 37 °C, RPMI 1640 containing 10% FBS was used. Stimulated with the compounds 6° and 6q to be tested for caspase-3, caspase-7, and caspase-9; Bax or Bcl2 and lysed with cell extraction buffer. To dilute the lysate over the range of the assay and measure human active caspase-3, caspase-7, caspase-9, Bax or Bcl2 content, Standard Diluent Buffer was used (BIORAD iScriptTM One-Step Real-Time RT-PCR Kit with SYBR® Green). The procedure for the used kit was in accordance with the manufacturer's instructions [38].

4.2.4.2. mRNA isolation. RNeasy extraction kit was used to isolate m RNA in up to 1 × 10^7 cells. RNeasyLysisBuffer (RLT) was used to disrupt and homogenize cells. Ethanol was added to the lysate to promote selective binding of RNA to the RNeasy membrane. The sample was applied to the RNeasy Mini spin column until total RNA bounds to the membrane. High quality of RNA was eluted by the action of RNase-free water. All binds were centrifuged using a micro-centrifuge [38].

4.2.4.3. Preparation of master mix and amplification protocol. A reaction mix of total volume (50 μL) was prepared according to the following recipe: 2X SYBR®Green RT-PCR Master (25 μL), forward primer (10 μM) (1.5 μL), reverse primer (10 μM) (1.5 μL), Nuclease-free H_2O (11 μL), RNA template (1 pg−100 ng total RNA) (10 μL) and iScriptreverse transcriptase for One-Step RT-PCR (1 μL).

Amplification was performed using 7500 Fast RT-PCR Systems (AppliedBiosystems, USA) 10 ng of cDNA using a Power Sybr Green PCR Master MIX (Applied Biosystems).The amplification protocol was as follows: cDNA synthesis: 50 °C for 10 min, iScript Reverse transcriptase inactivation: 95 °C for 5 min, polymerase chain reaction cycling and detection (40 cycles): 95 °C for 10 s, data collection step: 60 °C for 30 s, melt curve analysis: 95 °C for 1 min, 55 °C for 1 min and 55 °C for 10 s (80 cycles, increasing each by 0.5 °C each cycle). Dissociation curve software was used to check the products routinely [38].

4.2.5. In vitro EGFR/HER2 inhibitory activity assay

A cell-free assay was performed to measure the percentage of inhibition of EGFR T790M and HER2 kinases according to the reported method. The used kit for immune-assay was cloud clone SEA757Hu 96 Tests. The following equation: E (%) = E max/(1+ [I]/ID_{50}) was applied, where E (%) is the fraction of the enzyme activity measured in the presence of the inhibitor, E max is the activity in the absence of the inhibitor, [I] is the inhibitor concentration and ID_{50} is the inhibitor concentration at which E (%) = 0.5 E max, then a dose-response curve was generated. For each experiment, mean values of two independent replicates were calculated [38].

4.2.6. In vivo anticonvulsant study

4.2.6.1. Animals. One hundred and ten male mice weighing (20–30 g) were received from the animal facility at Faculty of Medicine (Kasr Al-Aini), Cairo University, Egypt. Mice were adapted to laboratory conditions for two weeks before the start of the experimental work, they were housed in large wire mesh cages (5 per cage) under standard laboratory conditions with temperature (24 ± 2 °C), humidity (about 60–70%), 12 h of dark/light cycle and free access to food and tap water. All animal dealings were in respect to the National Institutes of Health (NIH) guide for the care and use of laboratory animals (NIH Publications No. 8023, revised 1978).

4.2.6.2. Experimental design. After the accommodation period, mice were randomly arranged into twenty two groups (five mice in each group) as follows:

Group 1 (Normal control group): Mice administered orally 1 ml distilled water daily for 10 days.
Group 2 (Status Epilepticus (SE) untreated model group): in which lithium-pilocarpine mice model of *Status Epilepticus* was induced (Lithium Carbonate (LiCa)/pilocarpine) where SE was induced according to the lithium-pilocarpine SE model [39,40]. Briefly, mice were administered pilocarpine hydrochloride powder (300 mg/kg i.p.; El-Gomhouria Co. for trading chemicals, Cairo, Egypt) 2 h after LiCa injection (3 mEq/kg i.p.; Nile Pharma Co. for Pharmaceuticals and Chemical Industries, Cairo, Egypt). In addition, mice were injected with atropine sulfate powder (1 mg/kg i.p.; Fluka (Chemika, Switzerland). 30 min prior to pilocarpine administration to reduce its peripheral cholinergic side effects.
Group (3) (phenytoin + SE): Mice received oral phenytoin (Nile Pharma Co. Cairo, Egypt) at a dose of (20 mg/kg).
Group (4) (lamotrigene + SE): Mice were given oral lamotrigine (GlaxoSmithKline Co. Cairo, Egypt) at a dose of (20 mg/kg).

Groups (5–22 group) (tested compounds + SE): Mice were administered orally the tested compounds **6a, 6b, 6c, 6d, 6e, 6f, 6g, 6h, 6i, 6j, 6k, 6L, 6m, 6n, 6o, 6p, 6q** and **6r** respectively at a dose of (20 mg/kg).

All drugs and tested compounds were given to mice for 10 days before induction of *Status Epilepticus*. After induction of SE in the groups administered phenytoin, lamotrigine and tested compounds, mice were continuously monitored to detect signs of seizure activity. Then mice in all groups were anesthetized by urethane (1 g/kg) for Electroencephalography (EEG) recording, using (AD Instruments Power Lab v.7.3.7) followed by offline analysis of EEG waves that illustrated and stored in a PC through the lab Chart program software.

After completion of EEG recording, mice were fasted overnight for 12 h and sacrificed by decapitation, then brains were rapidly dissected, weighed and stored in −80 °C in Medical Biochemistry and Molecular Biology Department, Kasr Al-Aini, Cairo University for further biochemical analysis of Malondialdehyde (MDA), reduced glutathione (GSH), gamma-aminobutyric acid (GABA) and glutamate in brain tissue.

4.2.6.3. Biochemical analysis. MDA [41] and GSH [42] were obtained from Biodiagnostic Co. (Giza, Egypt), and measured calorimetrically in the brain tissue. GABA was available from (Bioassay Technology Laboratory) and Glutamate (obtained from (CusaBio co.) both were assessed in the brain tissue using ELISA kits based on manufacturer's protocol.

4.2.6.4. Statistical analysis. All obtained data were expressed as mean ± SD. Statistical analysis was achieved by using one-way ANOVA followed by Tukey post-hoc test by the aid of the computer software program SPSS 22 (SPSS, Chicago, Ill, USA), where the value of $p < 0.05$ was regarded as statistically significant.

4.3. ADME study

4.3.1. In silico ADME prediction

In order to predict pharmacokinetic properties for test compounds, PreADME online server (https://preadmet.bmdrc.kr/) was used. Many characters were calculated such as human intestinal absorption (HIA), cell permeability of CaCo-2 cell and Maden Darby Canine Kideny (MDCK) cell, plasma protein binding (PPB), blood brain barrier (BBB) and skin permeability (SP). The obtained results were listed in Table 9.

4.3.2. Predicted pharmacokinetic properties

Bioactivity properties such as G-protein coupling receptor (GPCR) ligand, ion channel modulator, kinase inhibitor, nuclear receptor ligand, protease inhibitor and enzyme inhibitor of compounds **6o** and **6q** and lapatinib were checked using molinspiration (https://www.molinspiration.com/). The obtained results were listed in Table 10.

Contribution

All authors contributed equally to this work.

Declaration of competing interest

The authors declare that they have no known competing financial interests or personal relationships that could have appeared to influence the work reported in this paper.

References

[1] P.B. Jensen, T. Hunter, Oncogenic kinase signalling, Nature 411 (2001) 355–365, https://doi.org/10.1038/35077225.
[2] S. Sogabe, Y. Kawakita, S. Igaki, H. Iwata, H. Miki, D.R. Cary, T. Takagi, S. Takagi, Y. Ohta, T. Ishikawa, Structure-based approach for the discovery of pyrrolo [3,2-*d*]pyrimidine-based EGFR T790M/L858R mutant Inhibitors, ACS Med. Chem. Lett. 4 (2013) 201–205, https://doi.org/10.1021/ml300327z.
[3] S.E.-S. Abbas, E.I. Aly, F.M. Awadallah, W.R. Mahmoud, 4-Substituted-1-phenyl-1μμ*H*-pyrazolo[3,4-*d*]pyrimidine derivatives: design, synthesis, antitumor and EGFR tyrosine kKinase inhibitory activity, Chem. Biol. Drug Des. 85 (2015) 608–622, https://doi.org/10.1111/cbdd.12451. Epub 2014 Nov 14.
[4] H. Shi, W. Zhang, Q. Zhi, M. Jiang, Lapatinib resistance in HER2+ cancers: latest findings and new concepts on molecular mechanisms, Tumor Biol. 37 (2016) 15411–15431, https://doi.org/10.1007/s13277-016-5467-2.
[5] F. Ciardiello, G. Tortora, EGFR Antagonists in cancer treatment, N. Engl. J. Med. 358 (2008) 1160–1174, https://doi.org/10.1056/NEJMra0707704.
[6] N.E. Hynes, H.A. Lane, ERBB receptors and cancer: the complexity of targeted inhibitors, Nat. Rev. Canc. 5 (2005) 341–354, https://doi.org/10.1038/nrc1609.
[7] A. Citri, Y. Yarden, EGF-ERBB signalling: towards the systems level, Nat. Rev. Mol. Cell Biol. 7 (2006) 505–516, https://doi.org/10.1038/nrm1962.
[8] S.N. Milik, A.K. Abdel-Aziz, D.S. Lasheen, R.A.T. Serya, S. Minucci, K.A.M. Abouzid, Surmounting the resistance against EGFR inhibitors through the development of thieno[2,3-*d*]pyrimidine-based dual EGFR/HER2

inhibitors, Eur. J. Med. Chem. 155 (2018) 316–336, https://doi.org/10.1016/j.ejmech.2018.06.011.
[9] E.K. Rowinsky, The erbB family: targets for therapeutic development against cancer and therapeutic strategies using monoclonal antibodies and tyrosine kinase inhibitors, Annu. Rev. Med. 55 (2004) 433–457, https://doi.org/10.1146/annurev.med.55.091902.104433.
[10] Cancer Research UK, The 10 Most Common Causes of Cancer Death, World, 2012 Estimates, 2014. http://www.cancerresearchuk.org/healthprofessional/cancer-statistics/worldwide-cancer/mortality#ref1. accessed June 1, 2017.
[11] S. Kamath, J.K. Buolamwini, Targeting EGFR and HER-2 receptor tyrosine kinases for cancer drug discovery and development, Med. Res. Rev. 26 (2006) 569–594, https://doi.org/10.1002/med.20070.
[12] E.L. Stewart, S.Z. Tan, G. Liu, M. Tsao, Known and putative mechanisms of resistance to EGFR targeted therapies in NSCLC patients with EGFR mutations — a review, Transl, Lung Canc. Res. 4 (2015) 67–81, https://doi.org/10.3978/j.issn.2218-6751.2014.11.06.
[13] K. Takezawa, V. Pirazzoli, M.E. Arcila, C.A. Nebhan, X. Song, E. de Stanchina, K. Ohashi, Y.Y. Janjigian, P.J. Spitzler, M.A. Melnick, G.J. Riely, M.G. Kris, V.A. Miller, M. Ladanyi, K. Politi, W. Pao, HER2 Amplification: a potential mechanism of acquired resistance to EGFR inhibition in EGFR-mutant lung cancers that lack the second-site EGFR T790M mutation, Canc. Discov. 2 (2012) 922–933, https://doi.org/10.1158/2159-8290.CD-12-0108.
[14] J. Engel, S. Smith, J. Lategahn, H.L. Tumbrink, L. Goebel, C. Becker, E. Hennes, M. Keul, A. Unger, H. Muller, M. Baumann, C.S. Fademrecht, G. Gunther, J.G. Hengstler, D. Rauh, Structure-guided development of covalent and mutant-selective pyrazolopyrimidines to target T790M Drug Resistance in epidermal growth factor receptor, J. Med. Chem. 60 (2017) 7725–7744, https://doi.org/10.1021/acs.jmedchem.7b00515.
[15] S.J. Kaspersen, J. Han, K.G. Nørsett, L. Rydså, E. Kjøbli, S. Bugge, G. Bjørkøy, E. Sundby, B. HelgeHoff, Identification of new 4-*N*-substituted 6-aryl-7*H*-pyrrolo[2,3-*d*] pyrimidine-4-amines as highly potent EGFR-TK inhibitors with Src-family activity, Eur. J. Pharmaceut. Sci. 59 (2014) 69–82, https://doi.org/10.1016/j.ejps.2014.04.011.
[16] D. Li, L. Ambrogio, T. Shimamura, S. Kubo, M. Takahashi, L.R. Chirieac, R.F. Padera, G.I. Shapiro, A. Baum, F. Himmelsbach, W.J. Rettig, M. Meyerson, F. Solca, H. Greulich, K.-K. Wong, BIBW2992, an irreversible EGFR/HER2 inhibitor highly effective in preclinical lung cancer models, Oncogene 27 (2008) 4702–4711, https://doi.org/10.1038/onc.2008.109.
[17] C.-H. Yun, K.E. Mengwasser, A.V. Toms, M.S. Woo, H. Greulich, K.-K. Wong, M. Meyerson, M.J. Eck, The T790M mutation in EGFR kinase causes drug resistance by increasing the affinity for ATP, Proc. Natl. Acad. Sci. 105 (2008) 2070–2075, https://doi.org/10.1073/pnas.0709662105.
[18] C. Carmi, E. Galvani, F. Vacondio, S. Rivara, A. Lodola, S. Russo, S. Aiello, F. Bordi, G. Costantino, A. Cavazzoni, R. Alfieri, A. Ardizzoni, P.G. Petronini, M. Mor, Irreversible inhibition of epidermal growth factor receptor activity by 3 aminopropanamides, J. Med. Chem. 55 (2012) 2251–2264, https://doi.org/10.1021/jm201507x.
[19] A.O. Walter, R.T. Sjin, H.J. Haringsma, K. Ohashi, J. Sun, K. Lee, A. Dubrovskiy, M. Labenski, Z. Zhu, Z. Wang, M. Sheets, T. St Martin, R. Karp, D. van Kalken, P. Chaturvedi, D. Niu, M. Nacht, R.C. Petter, W. Westlin, K. Lin, S. Jaw-Tsai, M. Raponi, T. Van Dyke, J. Etter, Z. Weaver, W. Pao, J. Singh, A.D. Simmons, T.C. Harding, A. Allen, Discovery of a mutant-selective covalent inhibitor of EGFR that overcomes T790M-mediated resistance in NSCLC, Canc. Discov. 3 (2013) 1404–1415, https://doi.org/10.1158/2159-8290.CD-13-0314. Epub 2013 Sep. 24.
[20] D.A. Cross, S.E. Ashton, S. Ghiorghiu, C. Eberlein, C.A. Nebhan, P.J. Spitzler, J.P. Orme, M.R. Finlay, R.A. Ward, M.J. Mellor, G. Hughes, A. Rahi, V.N. Jacobs, M.R. Brewer, E. Ichihara, J. Sun, H. Jin, P. Ballard, K. Al-Kadhimi, R. Rowlinson, T. Klinowska, G.H. Richmond, M. Cantarini, D.W. Kim, M.R. Ranson, W. Pao, AZD9291, an Irreversible EGFR TKI, overcomes T790M-mediated resistance to EGFR inhibitors in lung cancer, Canc. Discov. 4 (2014) 1046–1061, https://doi.org/10.1158/2159-8290.CD-14-0337.
[21] K. Dhingra, Rociletinib: has the TIGER lost a few of its stripes? Ann. Oncol. 27 (2016) 1161–1164, https://doi.org/10.1093/annonc/mdw140.
[22] N. Van Der Steen, C. Caparello, C. Rolfo, P. Pauwels, G.J. Peters, E. Giovannetti, New developments in the management of nonsmall- cell lung cancer, focus on rociletinib: what went wrong? OncoTargets Ther. 9 (2016) 6065–6074, https://doi.org/10.2147/OTT.S97644.
[23] S.L. Greig, Osimertinib: first global approval, Drugs 76 (2016) 263–273, https://doi.org/10.1007/s40265-015-0533-4.
[24] P.A. Janne, J.C.H. Yang, D.W. Kim, D. Planchard, Y. Ohe, S.S. Ramalingam, M.J. Ahn, S.W. Kim, W.C. Su, L. Horn, D. Haggstrom, E. Felip, J.H. Kim, P. Frewer, M. Cantarini, K.H. Brown, P.A. Dickinson, S. Ghiorghiu, M. Ranson, AZD9291 in EGFR inhibitor-resistant non-small-cell lung cancer, N. Engl. J. Med. 372 (2015) 1689–1699, https://doi.org/10.1056/NEJMoa1411817.
[25] H. Irannejad, H. Nadri, N. Naderi, S.N. Rezaeian, N. Zafari, A. Foroumadi, M. Amini, M. Khoobi, Anticonvulsant activity of 1,2,4-triazine derivatives with pyridyl side chain: synthesis, biological, and computational study, Med. Chem. Res. 24 (2015) 2505–2513, https://doi.org/10.1007/s00044-014-1315-3.
[26] B.P. Mallikarjuna, G.V.S. kumar, Sastry, J. Nagara, K.P. Manohara, Synthesis and anticonvulsant activity of some potent 5,6-bis aryl 1,2,4-triazines, Zhejiang Univ. Sci. B 8 (2007) 526–532, https://doi.org/10.1631/jzus.2007.B0526.
[27] A.N. Prasad, C. Prasad, in: J.M. Pellock, B.F. Bourgeols, W.E. Dodson (Eds.), Pediatric Epilepsy: Diagnosis and Therapy, third ed., Demos Publishers, New York, 2001, p. 117.
[28] M.M. Acharya, B. Hattiangady, A.K. Shetty, Progress in neuroprotective strategies for preventing epilepsy, Prog. Neurobiol. 84 (2008) 363–404, https://doi.org/10.1016/j.pneurobio.2007.10.010.
[29] S. Shorvon, E. Perucca, J. Engel Jr. (Eds.), The Treatment of Epilepsy, third ed., Wiley-Blackwell, Oxford, 2009, p. 123.
[30] M. Bialer, S.I. Johannessen, H.J. Kupferberg, R.H. Levy, E. Perucca, T. Tomson, Progress report on new antiepileptic drugs: a summary of the Seventh Eilat Conference (EILAT VII), Epilepsy Res. 61 (2004) 1–148, https://doi.org/10.1016/j.eplepsyres.2004.07.010.
[31] M. Amir, I. Ali, M.Z. Hassan, N. Mulakayala, Design, synthesis, and biological evaluation of hydrazine incorporated 1,2,4-triazines as anticonvulsant agents, Arch. Pharm. Chem. Life Sci. 347 (2014) 1–11, https://doi.org/10.1002/ardp.201400045.
[32] A.S. El-Azab, K.E.H. ElTahir, Synthesis and anticonvulsant evaluation of some new 2,3,8-trisubstituted-4(3*H*)-quinazoline derivatives, Bioorg. Med. Chem. Lett 22 (2012) 327–333, https://doi.org/10.1016/j.bmcl.2011.11.007.
[33] D. Kaushik, S.A. Khan, G. Chawla, S. Kumar, *N*′-[(5-chloro-3-methyl-1-phenyl-1*H*-pyrazol-4-yl)methylene] 2/4-substituted hydrazides: synthesis and anticonvulsant activity, Eur. J. Med. Chem. 45 (2010) 3943–3949, https://doi.org/10.1016/j.ejmech.2010.05.049.
[34] D.S. Danny, H.L. René, L.S. Jill, V. Alan, Comparative anticonvulsant potency and pharmacokinetics of (+)- and (−)-enantiomers of stiripentol, Epilepsy Res. 1 (1992) 29–36, https://doi.org/10.1016/0920-1211(92)90088-B.
[35] M.M. Kandeel, S.M. Ali, E.K.A. Abed ElALL, M.A. Abdelgawad, P.F. Lamie, Synthesis and antitumor activity of novel pyrazolo[3,4-*d*]pyrimidin-4(5*H*)-one derivatives, J. Chem. Pharmaceut. Res. 4 (2012) 4097–4106.
[36] A. Rahmouni, A. Romdhane, A. Ben said, V.G. rineau, D. Touboul, H. Ben Jannet, Synthesis of novel isoxazolines and isoxazoles of *N*-substituted pyrazolo[3,4-*d*]pyrimidin-4(5*H*)-one derivatives through [3+2] cycloaddition, Arab. J. Chem. 12 (2019) 1974–1982, https://doi.org/10.1016/j.arabjc.2014.10.053.
[37] P.F. Lamie, J.N. Philoppes, L. Rárová, Design, synthesis, and biological evaluation of novel 1,2-diaryl-4-substituted-benzylidene-5(4*H*)-imidazolone derivatives as cytotoxic agents and COX-2/LOX inhibitors, Arch. Pharm. Chem. Life Sci. 351 (2018) 1700311–1700322, https://doi.org/10.1002/ardp.201700311.
[38] J.N. Philoppes, P.F. Lamie, Design and synthesis of new benzoxazole/benzothiazole-phthalimide hybrids as antitumor-apoptotic agents, Bioorg. Chem. 89 (2019) 102978, https://doi.org/10.1016/j.bioorg.2019.102978.
[39] E.D. Martín, M.A. Pozo, Animal models for the development of new neuropharmacological therapeutics in the *Status Epilepticus*, Curr. Neuropharmacol. 4 (2006) 33–40, https://doi.org/10.2174/157015906775203002.
[40] M. Glien, C. Brandt, H. Potschka, H. Voight, U. Ebert, W. Loscher, Repeated low dose treatment of rats with pilocarpine: low mortality but high proportion of rats developing epilepsy, Epilepsy Res. 46 (2001) 111–119, https://doi.org/10.1016/s0920-1211(01)00272-8.
[41] H. Ohkawa, W. Ohishi, K. Yagi, Assay for lipid peroxides in animal tissues by thiobarbituric acid reaction, Anal. Biochem. 95 (1979) 351–358, https://doi.org/10.1016/0003-2697(79)90738-3.
[42] E. Beutler, O. Duron, M.B. Kelly, Improved method for the determination of glutathione, J. Lab. Clin. Med. 61 (1963) 882–888. PMID: 13967893.